71-25,267

EMARA, Mostafa Mahmoud, 1942-
ULTRASONIC ABSORPTION STUDY OF €-CAPROLACTAM IN CYCLOHEXANE SOLUTIONS.

University of Maryland, Ph.D., 1971
Chemistry, physical

University Microfilms, A XEROX Company, Ann Arbor, Michigan

© 1971

MOSTAFA MAHMOUD EMARA

ALL RIGHTS RESERVED

ULTRASONIC ABSORPTION STUDY OF ε-CAPROLACTAM IN CYCLOHEXANE SOLUTIONS

by
Mostafa Mahmoud Emara

Thesis submitted to the Faculty of the Graduate School
of the University of Maryland in partial fulfillment
of the requirements for the degree of
Doctor of Philosophy
1971

Qq1

APPROVAL SHEET

Title of Thesis: Ultrasonic Absorption Study of ε-Caprolactam in Cyclohexane Solutions

Name of Candidate: Mostafa Mahmoud Emara
Doctor of Philosophy, 1971

Thesis and Abstract Approved:

Gordon Atkinson
Professor of Chemistry
Department of Chemistry

Date Approved: 18 September, 1970

PLEASE NOTE:

Some pages have indistinct print. Filmed as received.

UNIVERSITY MICROFILMS.

ABSTRACT

Title of Thesis: Ultrasonic Absorption Study of ε-Caprolactam in Cyclohexane Solutions

Mostafa M. Emara, Doctor of Philosophy, 1971

Thesis directed by: Gordon Atkinson, Professor of Chemistry

The ultrasonic absorption technique was used to study the self-association of ε-caprolactam in cyclohexane at 6°C, 10°C, 17°C and 25°C. The experimental data were found to fit a single relaxation. This relaxation was due to the presence of chemical equilibrium between monomers and dimers of ε-caprolactam. It is shown that the best model to fit the data, consistent with other workers' results, is the formation of a cyclic dimer in a two-step process. The observed single relaxation was assigned to the first step, formation of the open dimer. Complete kinetic and equilibrium analysis of the first step was possible from the combination of the ultrasonic data and the overall equilibrium constant for the IR data. The equilibrium constants for the second step are also determined.

ACKNOWLEDGMENTS

The author wishes to extend his sincere gratitude to Professor Gordon Atkinson for his guidance, generous time and encouragement throughout this investigation.

The support of this research by the Army Research Office (Durham) under Grant DA-AROD-31-124-G818 and the Office of Saline Water, U. S. Department of the Interior, under Grant 14-01-0001-1656 is gratefully acknowledged. The computer time for this project was made available through National Aeronautics and Space Administration Grant NsG-398 to the Computer Science Center of the University of Maryland.

Thanks are extended to Mrs. Edna Juel for typing the dissertation.

The scholarship granted to the author by the U.A.R. government and the Fulbright fellowship in the early stages of my studies in the United States are greatly appreciated.

I wish to express personal gratitude to my wife, Nazik, and my parents for their continual encouragement and inspiration.

TABLE OF CONTENTS

Page

ACKNOWLEDGMENTS ii

LIST OF TABLES v

LIST OF FIGURES vii

CHAPTER I. LITERATURE SURVEY 1

Part 1. Equilibria 1

Part 2. Kinetics 5

CHAPTER II. THEORY 12

A. Relaxation Methods 12

B. Relaxation Time (τ) 13

C. Theory of Chemical Relaxation 13

D. Theory of Ultrasonic Absorption 21

E. Multi-step Process 28

F. The Cause for the Absorption of Sound Wave in a Fluid . . 29

CHAPTER III. EQUIPMENT AND EXPERIMENTAL PROCEDURE 31

A. Ultrasonic Equipment 31

B. Chemicals and Solutions 36

C. Experimental Procedure 37

CHAPTER IV. EXPERIMENTAL RESULTS AND DATA ANALYSIS 39

A. Evaluation of Absorption Coefficient, α, from Raw Data . . 39

B. Effect of Concentration 40

C. Effect of Temperature 41

D. Effect of Frequency 41

Page

E. Evaluation of Relaxation Parameters A, f_c and B 41

F. Calculation of Relaxation Time 46

CHAPTER V. MODELS 47

A. Previous Models Suggested in the Literature for Similar Systems 47

B. Proposed Models on the System under Investigation 51

CHAPTER VI. SUMMARY AND CONCLUSION 68

A. Summary 68

B. Conclusion 69

APPENDIX A. RELATION BETWEEN THE RELAXATION STRENGTH AND THERMODYNAMIC PARAMETERS 71

APPENDIX B. CALCULATION OF ABSORPTION COEFFICIENT (α) 76

APPENDIX C. CALCULATION OF A, B and f_c 80

APPENDIX D. TABULATED EXPERIMENTAL AND CALCULATED RESULTS 87

APPENDIX E. COMPUTER PROGRAM FOR THE TWO-PARAMETER FIT 95

LIST OF REFERENCES 97

LIST OF TABLES

Table		Page
I.	Thermodynamic functions for the Dissociation of Lactam Dimers	5
II.	Values of the Relaxation Parameters	46
III.	Rate Constants and Equilibrium Constants for One-Step Model	54
IV.	Equilibrium Concentrations of Monomer ε-Caprolactam in Cyclohexane	59
V.	Calculated τ_2^{-1} Obtained from the Two-Parameter Computer Program Fit	60
VI.	Rate Constants and Equilibrium Constants Obtained from the Two-Parameter Fit	60
VII.	Rate Constants of the First Step and Equilibrium Constants for the First and Second Steps Using Two-step Model	61
VIII.	Energies of Activation and Enthalpy Change for the First Step	63
IX.	Physical Constants of Pure Cyclohexane at 17°C	66
X.	Summary of the Kinetics and Equilibrium Constants for the Two-Step Model	69
XI.	Measured Absorption of Pure Cyclohexane at 10°C	87
XII.	Measured Absorption of Pure Solvents and ε-Caprolactam Solutions in Various Solvents at 25°C	88
XIII.	Measured and Calculated Absorption of .046 M ε-Caprolactam-Cyclohexane at 6°C	88

Table		Page
XIV.	Measured and Calculated Absorption of .094 M ε-Caprolactam-Cyclohexane at 6°C	89
XV.	Measured and Calculated Absorption of .15 M ε-Caprolactam-Cyclohexane at 6°C	89
XVI.	Measured and Calculated Absorption of .026 M ε-Caprolactam-Cyclohexane at 10°C	90
XVII.	Measured and Calculated Absorption of .05 M ε-Caprolactam-Cyclohexane at 10°C	90
XVIII.	Measured and Calculated Absorption of .103 M ε-Caprolactam-Cyclohexane at 10°C	91
XIX.	Measured and Calculated Absorption of .05 M ε-Caprolactam-Cyclohexane at 17°C	91
XX.	Measured and Calculated Absorption of .096 M ε-Caprolactam-Cyclohexane at 17°C	92
XXI.	Measured and Calculated Absorption of .15 M ε-Caprolactam-Cyclohexane at 17°C	92
XXII.	Measured and Calculated Absorption of .048 M ε-Caprolactam-Cyclohexane at 25°C	93
XXIII.	Measured and Calculated Absorption of .096 M ε-Caprolactam-Cyclohexane at 25°C	93
XXIV.	Measured and Calculated Absorption of .148 M ε-Caprolactam-Cyclohexane at 25°C	94

LIST OF FIGURES

Figure		Page
1.	Schematic structures of some aliphatic lactams	3
2.	Periodic perturbation of chemical equilibrium by external parameter	30
3a.	Ultrasonic cell	32
3b.	Components of Ultrasonic Cell	33
4.	Block Diagram of Ultrasonic Apparatus	34
5.	α/f^2 vs log f of ε-caprolactam in cyclohexane, 6°C	42
6.	α/f^2 vs log f of ε-caprolactam in cyclohexane, 10°C	43
7.	α/f^2 vs log f of ε-caprolactam in cyclohexane, 17°C	44
8.	α/f^2 vs log f of ε-caprolactam in cyclohexane, 25°C	45
9.	$1/\tau^2$ vs conc. of ε-caprolactam in cyclohexane, 25°C	53
10.	ln K_{IR} vs 1/T of ε-caprolactam in CCl_4 (Lord and Porro) . .	55
11.	τ_1^{-1} vs $\bar{A}$ of ε-caprolactam in cyclohexane	62
12.	ln η vs 1/T of cyclohexane	65

CHAPTER I

LITERATURE SURVEY

In this chapter a brief review of the equilibria and kinetics of hydrogen bonded systems in non-aqueous solvents will be presented. The systems reviewed are those solutes which have the tendency of self-association in organic solvents. The first part, which is divided into two sections, discusses the equilibria. In section one a review of equilibria between monomers and their associated molecules through the O-H - - - O type of H-bond is given. The second section of part one covers those equilibria involving the N-H - - - O type of H-bond.

Part 1. Equilibria

(a) O-H - - - O type of H-bond.

It has been known for almost a century that in dilute solutions of carboxylic acids in hydrocarbons or similar solvents[1,2] the monomer forms of these acids are in equilibrium with associated forms. A variety of techniques has been used to show this fact. Among such methods are freezing-point depression, vapor-pressure depression, boiling-point elevation and absorption spectroscopy.[3]

In most of the acids investigated the associated molecules were shown to be in a dimeric form. However, in contrast to the gas phase there is no direct evidence that the dimer is cyclic in solution.

The thermodynamics of self-association of alcohols and phenols in non-aqueous solvents has been quantitatively investigated in detail by means of NMR and IR techniques. Davis, Pitzer and Rao,[4] Rao[5] and Pople,

Bernstein and Schneider[6] among others have studied the steric and electronegativity effects on the strength of the hydrogen bonds in various alcohols and phenols. Their results showed that the hydrogen-bond energies in aliphatic alcohols are in the order methanol > ethanol > 2-propanol > t-butyl alcohol. It was also concluded from the non-hindered alcohol studies that dimers are the dominant form of associated molecules. In their evaluation of the equilibrium constants for the dimerization of alcohols and phenols, the cyclic structure of the dimer was assumed. In the hindered alcohols, however, there is a good possibility that the dimers are not cyclic. These authors and others seem to agree on the presence of dimer as the dominant associated form but don't agree on whether it is in the cyclic (I) or the open form (II).

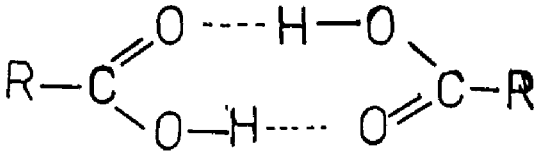

I. Cyclic Form

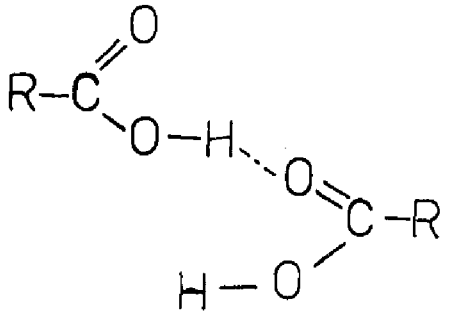

II. Open Form

(b) N-H - - - O type of H-bond.

Several investigators have studied the association of both amides and cyclic amides (lactams) in organic solvents in general and CCl_4 in particular. Most of these studies were carried out by infrared spectroscopy. Since this thesis deals mainly with ε-caprolactam-cyclohexane solutions, special attention will be given to equilibria studies of cyclic amides.

In 1951 M. Tsuboi[7,8] studied the molecular association of

δ-valerolactam (C_5H_9NO), Fig. 1b, in its carbon tetrachloride solutions by infrared spectroscopy. He found that this solute exhibits three N-H bands: 2.92μ (assigned to free molecules), 3.11μ (assigned to associated molecules), 3.24μ (also assigned to associated molecules). Measurements of the absorption intensities of two of these N-H bands (3.11μ and 3.24μ) were made with the objective of determining the concentrations of free and associated molecules in solutions of various concentrations at different temperatures.

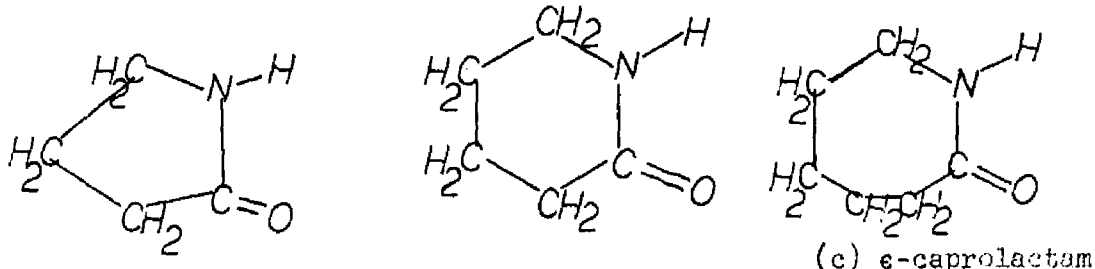

(a) γ-buterolactam (C_4H_7NO)

(b) δ-valerolactam (C_5H_9NO)

(c) ε-caprolactam ($C_6H_{11}NO$)

Fig. 1. Schematic structures of some aliphatic lactams.

From the results obtained the author concluded that a dimer coexists with monomers C_5H_9NO in equilibrium

$$2C_5H_9NO \rightleftarrows (C_5H_9NO)_2 \quad .$$

The values of enthalpy change (ΔH) and the entropy change (ΔS) accompanying the dimer formation in the solution were obtained as ΔH = -10.3 ± 1.0 Kcal/mol and ΔS = -23.5 ± 2.5 eu. He also concluded that the dimer was cyclic.

This conclusion did not quite agree with that of Dorman and Sutherland,[9] who studied the spectra of a similar cyclic amide (γ-buterolactam), Fig. 1a, in the same solvent. The latter authors attributed the two N-H associated bands exhibited by this compound to two different

types of associated molecules. However, in 1954 Pimentel and coworkers[10] studied the IR spectra of γ-buterolactam in CCl_4 and reached a conclusion similar to that of Tsuboi.

Later, in 1960, Lord and Porro[11] investigated the monomer-dimer equilibrium of ε-caprolactam ($C_6H_{11}NO$), Fig. 1c, in CCl_4 solution. From their IR spectrum studies they showed that this compound forms a hydrogen-bonded dimer. The equilibrium data were obtained at four temperatures and at various concentrations in the range between .000177 and .0354 mol/liter. When they studied the same system in the concentration range between .0177 and .354 mol/liter, the equilibrium constants were no longer constant. The authors also claimed that the dimer formed was in the cyclic form III and not the open form IV.

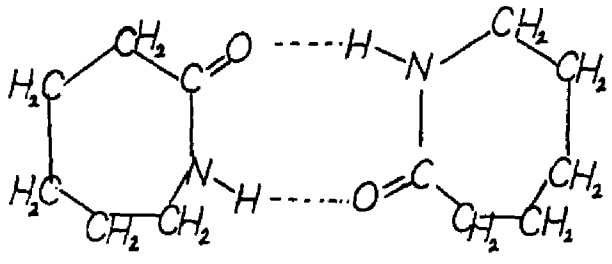

III

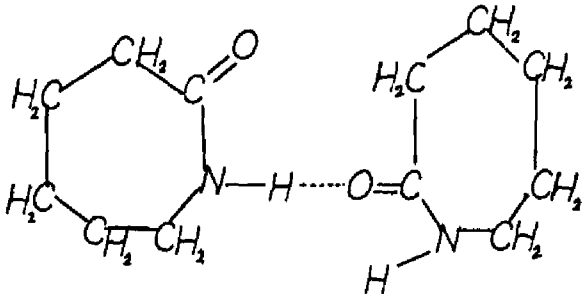

IV

They based this conclusion mainly on the value obtained for the enthalpy change ΔH° (5.46 ± .25 Kcal/mol) of the reaction. The investigators interpreted the non-constant values for the equilibrium constant at the higher concentration range (.0177-.354 mol/liter) as due to the possible existence of the open dimer IV.

Very recently Chen and Swenson[12,13] have made a thorough investigation on the self-association of the cis-lactams in CCl_4, dioxane, DMSO, H_2O and D_2O. δ-valerolactam-CCl_4 solutions were studied in the concentration range 3.31×10^{-3} - 5.29×10^{-3} mol/l. The enthalpy change was -5.93 Kcal/mol for the dimer formation and ΔS° = -10.8 cal/mole-deg.

From the results of their study on all the cis-lactams, it appears that the value of ΔH° for δ-valerolactam reported by Tsuboi is much too high. Tsuboi's value has been questioned previously by Lord and Porro. Table I contains the thermodynamic functions for the dissociation of lactam dimers, n = 5, 6, 7, 8. See V.

Table I. Thermodynamic functions for the Dissociation of Lactam Dimers

Ring Size	C x 10^3 Mol/l	ΔH° Kcal/mol	ΔS° Cal/mol-deg	ΔG°_{25} Kcal/mol
5	6.76 - 7.66	6.37 ± 0.10	11	2.97
6	7.04 - 8.05	5.90 ± 0.09	11	2.74
7	6.62 - 8.02	5.52 ± 0.05	10	2.54
8	6.28 - 8.09	6.33 ± 0.14	13	2.57

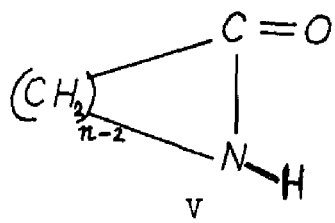

V

Part 2. Kinetics

Kinetic studies, in general, enable us to investigate the mechanisms of reactions as well as determine the rates at which these reactions take place. However, kinetic studies of the above mentioned type of systems were difficult to do before the discovery of the relaxation techniques,[11] discussed later, because of the extreme rapidity of such reactions. Ultrasonic absorption has been the most common and successful technique among the relaxation methods for studying the kinetics of H-bonded systems.

(a) O-H - - - O type.

Historically, acetic and propionic acids were the first liquids in which ultrasonic relaxation was observed. It is known from earlier work that acetic acid forms double molecules united by two hydrogen bonds in both the vapor and the liquid phase, although the heat of reaction is only known reliably for the vapor phase and for dilute solutions in non-polar solvents. In 1956 Piercy and Lamb[14] measured the ultrasonic absorption of dilute solutions of acetic acid in chlorobenzene, nitrobenzene, n-hexane and toluene. The authors claimed that two relaxations were observed, one below 10 MHz and a second one at frequencies higher than 15 MHz. The higher relaxations were attributed to the perturbation of the monomer-dimer equilibrium. These same authors, however, were not able to explain the relaxation in the lower frequency region.

In 1960 Maier[15,16] studied the ultrasonic absorption of benzoic acid in different organic solvents. The solvents used were CCl_4, cyclohexane, benzene, toluene, chlorobenzene and chloroform. The measurements were made at two temperatures, 20° and 40°C, and at concentrations between .2 mole % and 2 mole %. The author analyzed his data on the basis of a single relaxation due to the perturbation of monomer-dimer equilibrium. Rassing, Østerberg and Bak[17] measured the ultrasonic absorption of benzoic acid, p-chlorobenzoic acid, p-methoxybenzoic acid, p-fluorobenzoic acid and p-methylbenzoic acid dissolved in dimethylformamide at 25°C. The authors have determined the rate constants for association and dissociation reactions of all these acids in dimethylformamide assuming monomer-dimer equilibria. They did not, however, exclude the possibility of the solvent-monomer interaction through H-bonding, but did not include it in their calculations.

Although several alcohols were measured thermodynamically, very few cases were studied kinetically. t-butyl alcohol in cyclohexane was studied by means of ultrasonic absorption. Musa and Eisner[18] claimed that the observed single relaxation fitted to a monomer-tetramer equilibrium. Tetramer seems to be unlikely in this particular case because of the steric effects in that alcohol. Goodman[19] re-analyzed their results and interpreted it in terms of monomer-dimer equilibrium and non-ideality of the system. Recently Garland and Atkinson studied[20] the same system by ultrasonics to clarify the association behavior. Both the experimental technique and the calculations of the latter authors have advantages over those of Musa and Eisner. Garland and Atkinson were able to analyze their results on the basis of monomer-dimer equilibrium. Again the type of dimer, cyclic or open, is not yet clear. Ultrasonic absorption studies of several other alcohols in aqueous solutions have been carried out. Such systems are of great importance in the understanding of the structure of water and effect of nonelectrolytes on it. However, these systems will not be discussed here since we are mainly concerned with self-association in non-aqueous systems.

(b) <u>N-H - - - O type</u>.

Association through this type of hydrogen bond, the peptide linkage, has been of great interest to many chemists. The reason for its importance is that many biological molecules such as peptides and proteins have this type of bonding. As mentioned earlier, equilibrium studies of this type started as early as in the 1940's. Kinetic studies on such systems, however, were not carried out before 1960. In this section a review of these studies is attempted.

In 1963 Bergman, Eigen and De Maeyer[21] studied ε-caprolactam in CCl_4

and in benzene solutions at 22°C by the dielectric relaxation technique. The measurements were made in the frequency range between 10 and 50 MHz and concentration range .0034 to .338 M in CCl_4 and .0107 M to .686 M in benzene solutions. They observed one relaxation which was attributed to the perturbation of the equilibrium

$$2X \underset{k_{21}}{\overset{k_{12}}{\rightleftharpoons}} X_2 \qquad (1)$$

where X = the ε-caprolactam in monomer form

X_2 = the ε-caprolactam in the cyclic dimer form.

It should be mentioned here that the relaxation frequencies from their figures are clearly much higher than the actual range of the measurements made. When CCl_4 was used as a solvent, the rate constants were $k_{12} = 5.5 \times 10^9$ M^{-1} sec^{-1} and $k_{21} = 4.6 \times 10^7$ sec^{-1}, yielding an association equilibrium constant of 120 M^{-1}. When benzene was used as solvent, k_{12} and k_{21} were found to be 6.5×10^9 M^{-1} sec^{-1} and 2.6×10^8 sec^{-1}, respectively, yielding an association equilibrium constant of 25 M^{-1}. The authors then concluded that although the data did fit the above mechanism (1) another mechanism involving the formation of the cyclic dimer in two steps is also possible.

Hammes and Spivey[22] made a kinetic study of the hydrogen bond dimerization of 2-pyridone in dioxane, 50 wt % dioxane-CCl_4 and 1 wt % H_2O-dioxane. They concluded from their ultrasonic measurements that the two hydrogen bonds were formed simultaneously (2) once the two monomers

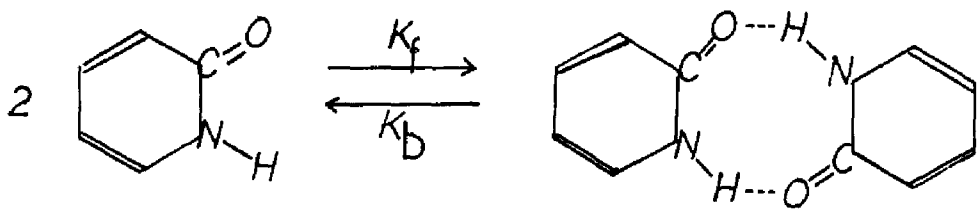

(2)

came close to each other. When the authors analyzed their data assuming the above mechanism, it fitted well when pure dioxane was the solvent. However, when the solvent was 50 wt % dioxane-CCl_4, some deviations were observed at low concentrations. They attributed these deviations from the proposed mechanism to non-ideality of the system. In this latter case they were not able to determine the rate constants directly from their data. Instead they assumed that the association step is diffusion controlled and the rate constant of the association was the same in all the solvents studied. The association rate constant in dioxane had the value 1.7×10^9 M^{-1} sec^{-1}. The value of the dissociation rate constant was found to be sensitive to the solvent and had values 9×10^8 sec^{-1}, $\sim 1.7 \times 10^8$ and 1.4×10^7 in pure dioxane, 1 wt % H_2O-dioxane and 50 wt % dioxane-CCl_4, respectively.

J. Rassing[23] has treated Hammes' data using the following 2-step mechanism:

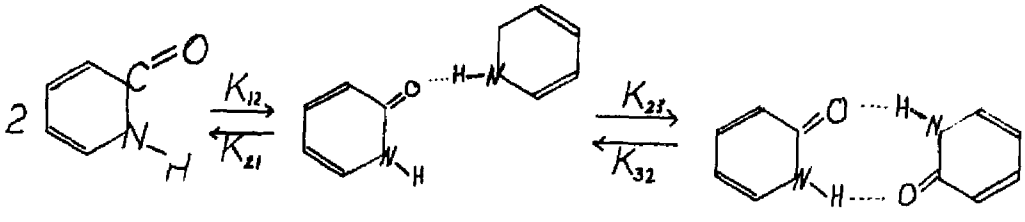

(3)

Using this model, he was able to calculate directly the forward rate constants of the first step from the data and also accounted for the deviation noticed in the case of 50 wt % dioxane-CCl_4 as solvent.

Recently Rassing and Østerberg[24] have made ultrasonic measurements in N-methyl acetamide, NMA, and dimethyl acetamide, DMA. They showed that in the frequency range investigated, 1 to 70 Mc, a relaxation was observed when they were mixed together in various proportions. The observed relaxation can be due to one of two possibilities, either an

internal rotation of the NMA molecule or an equilibrium between hydrogen-bonded chains. The first case was excluded by the authors on the basis of the non-linear dependence of the amplitudes of the ultrasonic absorption on the concentration. The equilibrium between monomers and associated polymers of NMA was represented by a large number of reaction steps. The observed relaxation was considered as a distribution of many relaxations close in time.

In 1968 Maeyer, Eigen and Suarez[25] investigated the kinetics of ε-caprolactam + 2-aminopyrimidine in cyclohexane. The dielectric dispersion method was used to study this system at 22°C. Two discrete relaxation processes were observed and were attributed to the dimerization of the lactam and to the formation of a 1:1 associate between ε-caprolactam and 2-aminopyrimidine. The higher relaxation was in the frequency range 40-80 MHz. The higher relaxation was assigned to the dimerization of the lactam, but no mention was made about the type of dimer. The lower one was assigned due to the 1:1 association between the two solutes. The mechanism proposed can be represented as follows:

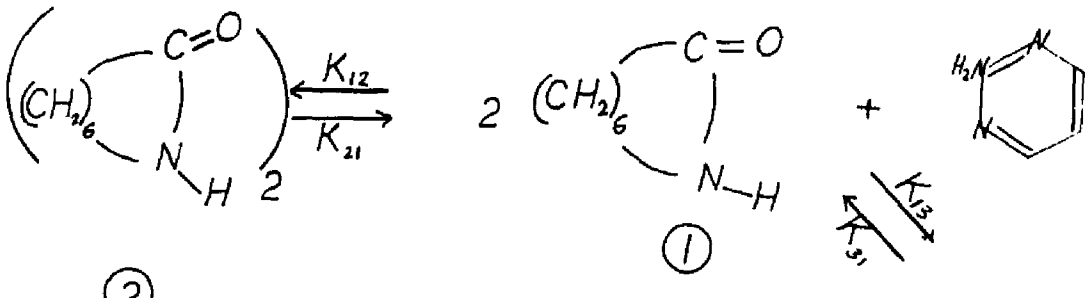

②

①

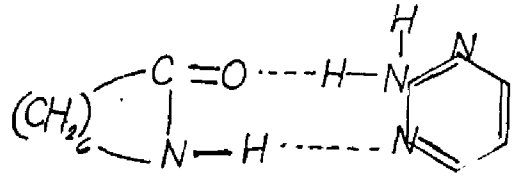

③

From the variation of the relaxation frequencies with concentrations the authors obtained the following results.

$$k_{12} = (4.8 \pm .2)10^{9}\ M^{-1}\ sec^{-1}$$

$$k_{21} = (3.0 \pm .2)10^{7}\ sec^{-1}$$

$$K' = k_{12}/k_{21} = 162 \pm 10\ M^{-1}$$

$$k_{13} = (7.9 \pm .2)10^{8}\ M^{-1}\ sec^{-1}$$

$$k_{31} = (1.1 \pm .2)10^{7}\ sec^{-1}$$

$$K'' = k_{13}/k_{31} = 70 \pm 5\ M^{-1}$$

where k_{ij} are the corresponding rate constants of the individual steps in the assigned mechanism and K', K'' are the equilibrium constants of the dimer and 1:1 complex formation respectively. From these results the authors concluded that the formation of hydrogen-bonded dimers of ε-caprolactam is diffusion controlled. A similar conclusion was made by Hammes and Spivey in the case of 2-pyridone-organic solvents systems and also by Garland and Atkinson in the case of the t-butanol-cyclo hexane system.

CHAPTER II

THEORY

An introduction to the relaxation methods is presented. The theory of chemical relaxation is applied to the two-step mechanism. In this treatment the rate equations are linearized and relaxation times are obtained as a function of the rate constants, equilibrium constants and stoichiometric concentrations. Finally, the theory of ultrasonic absorption is considered and the equation for a single relaxation is derived.

A. Relaxation Methods

Two decades ago chemists were only able to study the rate of solution reactions that were half completed in more than a millisecond. Now rates of reactions with half-lives as short as a few nanoseconds can be measured. This great progress has resulted from a new approach to the study of reaction rates, relaxation methods. In this approach the equilibrium of a chemical reaction is suddenly perturbed by a rapid change of some external parameter such as temperature or pressure. The subsequent shift from equilibrium, which proceeds with finite time lag, is then followed by direct or indirect observation. This basic principle was introduced in the early 1950's by Manfred Eigen[28] at Göttingen.

Several experimental methods using the above principle are the sound absorption method, the temperature jump method, the electric impulse method, and the pressure jump method.

The range of half lives accessible to one or another of the relaxation methods is from about 10^{-9} to over one sec. The method used in the

present work is ultrasonic absorption. In a following section the fundamental equations of that technique will be discussed. An important expression usually used in all the relaxation methods is the "relaxation time."

B. Relaxation Time (τ)

Suppose that the reaction whose rate we wish to measure is at equilibrium. If this equilibrium is disturbed by a sudden change of an external parameter, there will be a time lag while the system approaches the new position of equilibrium. This time lag takes place due to the fact that the rate constants have finite values. It is expressed as a relaxation time and can be related to the rate constants of the forward and reverse reactions. Such relationships, however, can be simple, as in the case of a single-step reaction, or complicated if the reaction involves multi-step processes.

C. Theory of Chemical Relaxation

1. Introduction.

Generally, in order to describe the relaxation behavior by a relaxation spectrum, sufficiently small perturbations have to be applied. In this case the rate equations can be linearized so that they may be solved by well-known mathematical operations. The theory of chemical relaxation of a reaction system comprising an arbitrary number of elementary processes involving many different reaction partners is reviewed in detail by several authors (Kustin,[27] Castellan,[28] Schwarz[29] and Czerlinski[30]). The following treatment is limited to the calculations of a three-state system consisting of two elementary reaction steps.

2. Reaction system and linearized rate equations.

Let us consider the two-step mechanism

$$A + A \underset{k_{21}}{\overset{k_{12}}{\rightleftharpoons}} A \text{ --- } A \underset{k_{32}}{\overset{k_{23}}{\rightleftharpoons}} A \text{ === } A \qquad (2.C.1)$$

(1) (2) (3)

where A is a monomer species; A --- A and A === A are dimer forms containing one and two hydrogen bonds respectively.

The classical rate equations for the above process are given by the following three equations.

$$-\frac{1}{2}\frac{d[A]}{dt} = k_{12}[A]^2 - k_{21}[A \text{ --- } A]$$

$$-\frac{d[A \text{ --- } A]}{dt} = k_{21}[A \text{ --- } A] - k_{12}[A]^2 + k_{23}[A \text{ --- } A] - k_{32}[A \text{ === } A]$$

$$-\frac{d[A \text{ === } A]}{dt} = k_{32}[A \text{ === } A] - k_{23}[A \text{ --- } A] \qquad (2.C.2)$$

When a small perturbation from the actual equilibrium takes place, there will be small changes between equilibrium concentrations and the actual concentrations, given by

$$\Delta A_1 = [A] - [\bar{A}]$$

$$\Delta A_2 = [A \text{ --- } A] - [\overline{A \text{ --- } A}]$$

$$\Delta A_3 = [A \text{ === } A] - [\overline{A \text{ === } A}] \qquad (2.C.3)$$

where ΔA_1, ΔA_2 and ΔA_3 are the concentration changes in states 1, 2 and 3; [A], [A --- A] and [A === A] are the actual concentrations of the various species in states 1, 2 and 3; and $[\bar{A}]$, $[\overline{A \text{ --- } A}]$ and $[\overline{A \text{ === } A}]$ are the equilibrium concentrations of the different species in the three states.

In the set of equations 2.C.3 the assumption is made that the equilibrium concentrations are time independent. Substituting for the actual concentrations from 2.C.3 into 2.C.2 we then get the set of equations

$$-\frac{1}{2}\frac{d}{dt}(\Delta A_1) = k_{12}([\bar{A}] + \Delta A_1)^2 - k_{21}([\overline{A\text{---}A}] + \Delta A_2)$$

$$= k_{12}[\bar{A}]^2 + 2k_{12}[\bar{A}]\Delta A_1 + k_{12}\Delta A_1^2 - k_{21}[\overline{A\text{---}A}] - k_{21}\Delta A_2$$

$$-\frac{d}{dt}(\Delta A_2) = k_{21}([\overline{A\text{---}A}] + \Delta A_2) - k_{12}([\bar{A}] + \Delta A_1)^2 + k_{23}([\overline{A\text{---}A}] + \Delta A_2) - k_{32}([\overline{A\text{=}A}] + \Delta A_3)$$

$$= k_{21}[\overline{A\text{---}A}] + k_{21}\Delta A_2 - k_{12}[\bar{A}]^2 - 2k_{12}[\bar{A}]\Delta A_1 - k_{12}\Delta A_1^2 + k_{23}[\overline{A\text{---}A}] + k_{23}\Delta A_2 - k_{32}[\overline{A\text{=}A}] - k_{32}\Delta A_3$$

and

$$-\frac{d}{dt}(\Delta A_3) = k_{32}([\overline{A\text{=}A}] + \Delta A_3) - k_{23}([\overline{A\text{---}A}] + \Delta A_2)$$

$$= k_{32}[\overline{A\text{=}A}] + k_{32}\Delta A_3 - k_{23}[\overline{A\text{---}A}] - k_{23}\Delta A_2 \qquad (2.C.4)$$

When we substitute for the equilibrium conditions 2.C.5

$$k_{12}[\bar{A}]^2 = k_{21}[\overline{A\text{---}A}]$$

$$k_{23}[\overline{A\text{---}A}] = k_{32}[\overline{A\text{=}A}] \qquad (2.C.5)$$

in the set of equations 2.C.4, retaining only the first-order terms, we get 2.C.6.

$$-\frac{d}{dt}(\Delta A_1) = 4k_{12}[\bar{A}]\Delta A_1 - 2k_{21}\Delta A_2$$

$$-\frac{d}{dt}(\Delta A_2) = -2k_{12}[\bar{A}]\Delta A_1 + [k_{21} + k_{23})\Delta A_2 - k_{32}\Delta A_3$$

and

$$-\frac{d}{dt}(\Delta A_3) = -k_{23}\Delta A_2 + k_{32}\Delta A_3 \qquad (2.C.6)$$

The above set of equations, 2.C.6, are called the linearized equations and can be represented in the following matrix form, 2.C.7.

$$\begin{pmatrix} \Delta\dot{A}_1 \\ \Delta\dot{A}_2 \\ \Delta\dot{A}_3 \end{pmatrix} = \begin{pmatrix} -4k_{12}[\bar{A}] & 2k_{21} & 0 \\ 2k_{12}[\bar{A}] & -(k_{21} + k_{23}) & k_{32} \\ k_{23} & -k_{32} & 0 \end{pmatrix} \begin{pmatrix} \Delta A_1 \\ \Delta A_2 \\ \Delta A_3 \end{pmatrix} \qquad (2.C.7)$$

where $\Delta\dot{A}_1$, $\Delta\dot{A}_2$ and $\Delta\dot{A}_3$ are the first derivative terms in 2.C.6.

The above set of equations 2.C.7 can be reduced to only two linearized equations by using the material balance equation 2.C.8

$$\Delta A_1 + 2\Delta A_2 + 2\Delta A_3 = 0 \qquad (2.C.8)$$

and the new set is represented in 2.C.9.

$$\Delta\dot{A}_1 + (4k_{12}[\bar{A}] + k_{21})\Delta A_1 + 2k_{21}\Delta A_3 = 0$$

$$\Delta\dot{A}_3 + 1/2k_{23}\Delta A_1 + (k_{23} + k_{32})\Delta A_3 = 0 \qquad (2.C.9)$$

If we now define

$$\begin{aligned} a_{11} &= 4k_{12}[\bar{A}] + k_{21} \\ a_{12} &= 2k_{21} \\ a_{21} &= 1/2k_{23} \\ a_{22} &= k_{23} + k_{32} \end{aligned} \qquad (2.C.10)$$

Equations 2.C.9 can be rewritten in the following form

$$\Delta\dot{A}_1 + a_{11}\Delta A_1 + a_{12}\Delta A_3 = 0$$

$$\Delta\dot{A}_3 + a_{21}\Delta A_1 + a_{22}\Delta A_3 = 0 \qquad (2.C.11)$$

3. Relaxation times as functions of concentrations and rate constants.

The relaxation times for the reaction mechanism 2.C.1 can be found by solving the eigen value problem for the matrix

$$\begin{Bmatrix} a_{11} & a_{12} \\ a_{21} & a_{22} \end{Bmatrix} \qquad (2.C.12)$$

which is simply done by setting the determinant of this matrix equal to zero

$$\begin{vmatrix} a_{11} - \lambda & a_{12} \\ a_{21} & a_{22} - \lambda \end{vmatrix} = 0 \qquad (2.C.13)$$

where λ is the eigen value and is equal to the reciprocal relaxation time.

Equation 2.C.13 can be represented in the familiar quadratic equation, 2.C.14,

$$\lambda^2 - (a_{11} + a_{22})\lambda + (a_{11}a_{22} - a_{12}a_{21}) = 0 \qquad (2.C.14)$$

the solution of which is

$$\frac{1}{\tau_{1,2}} = \lambda = \frac{1}{2}\left[(a_{11} + a_{22}) \pm \sqrt{(a_{11} + a_{22})^2 - 4(a_{11}a_{22} - a_{12}a_{21})}\right] . \qquad (2.C.15)$$

2.C.15 can be written as

$$\frac{1}{\tau_{1,2}} = \frac{1}{2}(a_{11} + a_{22})\left\{1 \pm \sqrt{1 - \frac{4(a_{11}a_{22} - a_{12}a_{21})}{(a_{11} + a_{22})^2}}\right\} \qquad (2.C.16)$$

In equation 2.C.16 one of the relaxation times corresponds to the plus sign of the square root, the other to the negative sign.

In order to express the above relaxation time in a less complicated manner for our use, two different cases will be considered.

a. τ_1 and τ_2 are nearly equal:

This case was treated by J. Rassing.[31] Let us rewrite equation 2.C.15 in the following form.

$$\frac{1}{\tau_{1,2}} = \frac{1}{2}\left\{(a_{11} + a_{22}) \pm \sqrt{(a_{11} - a_{22})^2 + 4a_{21}a_{12}}\right\} \qquad (2.C.17)$$

For the case under discussion, $\tau_1 \sim \tau_2$, the square root term can be neglected. Thus

$$\frac{1}{\tau_{1,2}} = \frac{1}{2}(a_{11} + a_{22}) \qquad (2.C.18)$$

Let $$N = a_{11}a_{22}/a_{21}a_{12} \quad \text{and} \quad N > 1 \tag{2.C.19}$$

$$\mathcal{E} = a_{11} - a_{22} \quad \text{and} \quad \mathcal{E} \ll a_{22} \tag{2.C.20}$$

$$K_2 = k_{23}/k_{32} \tag{2.C.21}$$

$$K_1 = k_{12}/k_{21} \tag{2.C.22}$$

Substituting in 2.C.18 for the values of a_{11}, a_{22}, a_{12} and a_{21} from 2.C.10 and then making use of 2.C.19, 2.C.20, 2.C.21 and 2.C.22, we obtain

$$\frac{1}{\tau_{1,2}} = \frac{1}{2}\left\{\left(k_{21}\frac{K_2N}{1+K_2} + k_{23}\frac{1+K_2}{K_2}\right) + \sqrt{\mathcal{E}^2 + 4k_{21}k_{23}}\right\} \tag{2.C.23}$$

and $$\mathcal{E} = \frac{k_{21}K_2}{1+K_2}N - \frac{k_{23}(1+K_2)}{K_2} \tag{2.C.24}$$

If the square root term is negligible compared to the other terms in 2.C.23 and if $1 + K_2 \sim K_2$ the reciprocal of the relaxation times then becomes

$$1/\tau_{1,2} = 2K_{12}[\bar{A}] + \Sigma/2 \tag{2.C.25}$$

where $$\Sigma = k_{21} + k_{23} + k_{32} \tag{2.C.26}$$

The equilibrium concentration $[\bar{A}]$ can be shown to be

$$[\bar{A}] = -\frac{k_{21}k_{32}}{4k_{12}(k_{23}+k_{32})} + \frac{k_{21}k_{32}}{4k_{12}(k_{32}+k_{23})}\sqrt{\frac{4k_{12}}{k_{21}k_{32}}(k_{32}+k_{23})A_o} \tag{2.C.27}$$

Substituting by $[\bar{A}]$ from 2.C.27 into 2.C.25, we have

$$1/\tau = R/2\left(-1 + \sqrt{\frac{4k_{12}A_o}{R} + 1}\right) + \Sigma/2 \tag{2.C.28}$$

where $$R = k_{21}k_{32}/k_{23} + k_{32} \tag{2.C.29}$$

and A_o is the stoichiometric concentration.

Equation 2.C.28 can be rewritten as

$$1/\tau + (R - \Sigma)/2 = \sqrt{k_{12}RA_o + R^2/4} \qquad (2.C.30)$$

Squaring both sides of 2.C.30, we get

$$1/\tau^2 + (R - \Sigma)1/\tau = k_{12}RA_o + \Sigma/4(2R - \Sigma) \qquad (2.C.31)$$

Equation 2.C.31 can take the following form:

$$(1/\tau)^2 + U(1/\tau) = VA_o + S \qquad (2.C.32)$$

where

$$U = R - \Sigma \qquad (2.C.33)$$

$$V = k_{12} R \qquad (2.C.34)$$

$$S = \Sigma/4(2R - \Sigma) \qquad (2.C.35)$$

Since $1/\tau$ increases with the concentration, if a wide range of concentration is studied, then the plot of $(1/\tau)^2$ vs A_o is linear at higher concentrations, where the term $U\ 1/\tau$ is small compared to $(1/\tau)^2$. At lower concentrations a curvature may be obtained. In this case the intercept can be positive or negative depending on the actual values of the rate constants involved. In the case of the formation of the dimer through one step the intercept must be positive always. For the two cases, however, the slope must be positive. A detailed discussion including both models will be given in Chapter V.

b. τ_1 is less than τ_2:

This condition implies that the first step is assumed to equilibrate rapidly compared to the second step, i.e., $a_{11}, a_{12} > a_{21}, a_{22}$.

If the square root term in equation 2.C.16 is expanded and only first non-vanishing terms are retained, we get

$$1/\tau_{1,2} = 1/2(a_{11} + a_{22}) \left\{ 1 \pm \left(1 - \frac{2(a_{11}a_{22} - a_{12}a_{21})}{(a_{11} + a_{22})^2} \right) \right\} \qquad (2.C.36)$$

Also under these conditions τ_1 and τ_2 can be separated in 2.C.36 and

$$1/\tau_1 = 1/2(a_{11} + a_{22}) \left[1 + \left[1 - \frac{2(a_{11}a_{22} - a_{12}a_{21})}{(a_{11} + a_{22})^2}\right]\right]$$

$$= 1/2(a_{11} + a_{22}) \left[2 - \frac{2(a_{11}a_{22} - a_{12}a_{21})}{(a_{11} + a_{22})^2}\right]$$

$$= (a_{11} + a_{22}) \left[1 - \frac{(a_{11}a_{22} - a_{12}a_{21})}{(a_{11} + a_{22})^2}\right] \qquad (2.C.37)$$

Since $1/\tau_1$ must be positive if it is real and measurable, then the inequality

$$\frac{a_{11}a_{22} - a_{12}a_{21}}{(a_{11} + a_{22})^2} < 1 \qquad (2.C.38)$$

must hold, and we obtain

$$1/\tau_1 = a_{11} + a_{22} \simeq a_{11}$$

$$1/\tau_1 = 4k_{12}\left[\bar{A}\right] + k_{21} \qquad (2.C.39)$$

The reciprocal of the τ_2 is also given by

$$1/\tau_2 = 1/2(4k_{12}[\bar{A}] + k_{21} + k_{23} + k_{32})$$

$$\left\{2 \frac{(4k_{21}[\bar{A}] + k_{21})(k_{23} + k_{32}) - k_{21}k_{23}}{(4k_{12}[\bar{A}] + k_{21} + k_{23} + k_{32})^2}\right\}$$

$$= \frac{(4k_{21}[\bar{A}] + k_{21})(k_{23} + k_{32}) - k_{21}k_{23}}{(4k_{12}[\bar{A}] + k_{21} + k_{23} + k_{32})} \qquad (2.C.40)$$

2.C.40 can be simplified to

$$1/\tau_2 = (k_{23} + k_{32}) - \frac{k_{23}}{4K_1[\bar{A}] + 1} \qquad (2.C.41)$$

It can be shown that

$$[\bar{A}] = \frac{-1 + \sqrt{1 + 8K_1(1 + K_2)A_o}}{4K_1(1 + K_2)} \qquad (2.C.42)$$

An overall equilibrium constant (K) is introduced and is given by

$$K = K_1(1 + K_2) \qquad (2.C.43)$$

Substituting 2.C.43 into 2.C.42 and then into 2.C.41, we have

$$1/\tau_2 = k_{23} + k_{32} - k_{23} \cdot \frac{-K_1 + K_1\sqrt{1 + 8KA_o}}{4K} + 1^{-1} \qquad (2.C.44)$$

or

$$1/\tau_2 = k_{23} + k_{32} - \frac{k_{23}k_{32}K}{k_{23} + k_{32}} \Phi(A_o) \qquad (2.C.45)$$

where

$$\Phi(A_o) = \frac{-1 + \sqrt{1 + 8KA_o}}{K} + \frac{1}{K_1}^{-1} \qquad (2.C.46)$$

In theory, according to this mechanism, two relaxations should be observed. Experimentally, however, depending on the frequency range of investigation and the amplitudes of both relaxations, two or one could be observed. Also, it should be noticed that τ_2 belongs to the slower step, while τ_1 belongs to the faster one.

D. Theory of Ultrasonic Absorption.

a. Wave Equation.

The ultrasonic technique is one of the relaxation methods and it involves the same general principle. The theory of a sound wave (obtaining the wave equation) propagating in fluids is based on three fundamental equations, namely: (1) the equation of continuity of mass flow, (2) Newton's second law, relating mass acceleration with force, and (3) an equation of state, i.e., $V = f(P,T)$.

The usual form of a wave equation can be obtained when these relations are linearized. A detailed discussion of the theory leading to obtaining and combining the above relations can be found in references 32 and 33. For the one-dimensional case of a plane sound wave propagating in the X-direction, the wave equation is represented by

$$\frac{\partial^2 P}{\partial t^2} - (1/\rho_o \beta_s) \frac{\partial^2 P}{\partial X^2} = 0 \qquad (2.D.1)$$

where P = the radiation pressure of the wave

X = the distance traveled by the wave from the sound source

ρ_o = density of the fluid

β_s = adiabatic compressibility

The velocity (v) of sound wave in a fluid is related to the density of the fluid and the adiabatic compressibility of the fluid by the following equation.

$$v = (1/\rho_o \beta_s)^{1/2} \qquad (2.D.2)$$

Assuming that the wave is a progressive adiabatic one and sinusoidal with time, a solution of equation 2.D.1 is given by

$$P = P_o \exp\{j\omega(t - X/v)\} \qquad (2.D.3)$$

where ω = angular frequency of the wave

$j = \sqrt{-1}$

b. Absorption Coefficient.

Equation 2.D.3 represents a progressive plane wave in a fluid where there is no loss of the energy of the wave due to any relaxation process. If, however, there is any process taking place to cause such loss of energy the pressure wave is described by

$$P = P_o \exp\{j\omega(t - X/v)\} \exp\{-\alpha X\} \qquad (2.D.4)$$

where α is described as the amplitude absorption coefficient.

c. Excess Absorption and Thermodynamics.

1. Introduction. In solutions chemists are usually interested in the excess absorption which is defined by the following relation

$$\alpha' = \alpha_{solution} - \alpha_{solvent} \qquad (2.D.5)$$

where $\alpha_{solution}$ and $\alpha_{solvent}$ are the absorption coefficients of the solution and the pure solvent respectively.

The solvent absorption, which is often called the classical absorption, is due to the combination of two effects. These are the viscosity and thermal conduction (see part f). In equation 2.D.5 $\alpha_{solvent}$ is taken as the absorption of pure solvent even in the presence of solute. This condition is not always true and account should be considered due to the effect of the solute on the absorption of the solvent. $\alpha_{solvent}$ may or may not be concentration dependent. The actual solvent absorption is taken as that measured at frequencies much higher than the frequency at which relaxation takes place.

A quantity which is often used in the representation of the ultrasonic data and is a measure of the excess absorption is the absorption per wave length, μ, given by

$$\mu = \alpha'\lambda \qquad (2.D.6)$$

where λ is the wave length of the wave, which is given by

$$\lambda = 2\pi v/\omega. \qquad (2.D.7)$$

2. Excess absorption and relaxation compressibility.[34] Since the ultrasonic wave is propagated adiabatically, a useful way to coordinate the wave and the chemical reaction is through the adiabatic compressibility.

The complex compressibility, β_s^*, can be presented by two terms, frequency independent β_{s_∞} and frequency dependent $\delta\beta_{s\omega}$.

$$\beta_s^* = \beta_{s_\infty} + \delta\beta_{s\omega} \tag{2.D.8}$$

which can be written as

$$\beta_s^* = \beta_s - \delta\beta_s + \frac{\delta\beta_s}{1 + j\omega\tau} \tag{2.D.9}$$

where $\beta_s = \beta_{s_\infty} + \delta\beta_s$

and $\delta\beta_{s\omega} = \delta\beta_s/1 + j\omega\tau$.

Rearranging 2.D.9 we then get

$$\beta_s^* = \beta_s - \frac{j\omega\tau\delta\beta_s}{1 + j\omega\tau} \quad . \tag{2.D.10}$$

Dividing both sides of 2.D.10 by β_s we get

$$[\beta_s^*/\beta_s] = 1 - \frac{\delta\beta_s}{\beta_s} \cdot \frac{j\omega\tau}{1 + j\omega\tau} \quad . \tag{2.D.11}$$

Also, the complex velocity of the sound wave can be represented by the following:

$$1/v^* = 1/v_\omega + \alpha/j\omega \tag{2.D.12}$$

where v^* = complex velocity

$v = v_\omega$ = the frequency dependent part of velocity

Equation 2.D.12 can be rewritten as

$$1/v^* = 1/v(1 - \alpha j v/2\pi f) \tag{2.D.13}$$

or

$$1/v^* = 1/v(1 - j\mu/2\pi) \tag{2.D.14}$$

where $\mu = \alpha v/f$.

Squaring both sides of equation 2.D.14

$$(1/v^*)^2 = (1/v)^2 \left\{1 + j^2\mu^2/4\pi^2 - j\mu/\pi\right\} \qquad (2.D.15)$$

Since in general $\mu < 2\pi$, equation 2.D.15 can be

$$(1/v^*)^2 = (1/v)^2 \left\{1 - j\mu/\pi\right\} \qquad (2.D.16)$$

Multiplying both sides by v^2

$$(v/v^*)^2 = 1 - j\mu/\pi \qquad (2.D.17)$$

From 2.D.2

$$v = [1/\rho_o\beta_s]^{1/2} \qquad (2.D.2)$$

Thus $\beta_s = 1/\rho_o v^2$ or $\beta_s^* = 1/\rho_o v^{*2}$ (2.D.18)

Using 2.D.17, 2.D.18 and 2.D.11 we then get

$$(v/v^*)^2 = \beta_s^*/\beta_s = 1 - \frac{j\omega\tau}{1 + j\omega\tau} \cdot \frac{\delta\beta_s}{\beta_s} \qquad (2.D.19)$$

Equating 2.D.17 and 2.D.19 the following relation can be obtained

$$\frac{j\mu}{\pi} = \frac{j\omega\tau}{1 + j\omega\tau} \cdot \frac{\delta\beta_s}{\beta_s} \qquad (2.D.21)$$

If we now let $\delta\beta_s = \beta_r$ = the compressibility due to the relaxation and let $\beta_s = \beta_o$ = the static compressibility, equation 2.D.21 becomes

$$\mu = \pi \frac{\omega\tau}{1 + \omega^2\tau^2} \cdot \frac{\beta_r}{\beta_o} \qquad (2.D.22)$$

Equation 2.D.21 relates, for a single relaxation process, the excess absorption per wave length to the compressibility.

It is clear that μ is a maximum when $\omega\tau = 1$. Therefore, the relaxation time can be found by finding the frequency at which excess absorption is a maximum.

Using the definition of excess absorption and equation 2.D.22, we can arrive at another useful expression often used in the treatment of

ultrasonic data.

$$\frac{\alpha'}{f^2} = \frac{2\pi^2}{v}\frac{\beta_r}{\beta_o}\frac{\tau}{1+\omega^2\tau^2} \qquad (2.D.22)$$

or $$\alpha/f^2 = \frac{2\pi^2}{v}\frac{\beta_r}{\beta_o}\frac{\tau}{1+\omega^2\tau^2} + (\alpha/f^2)_{\text{solvent}} \qquad (2.D.23)$$

where $(\alpha/f^2)_{\text{solvent}}$ includes solute and other effects.

In equations 2.D.21, 2.D.22 and 2.D.23 the ratio β_r/β_o is sometimes designated the relaxation strength and is related to the thermodynamic properties ΔH and ΔV of the reaction responsible for the relaxation process.

3. Relaxation strength and thermodynamic parameters.[34] An equation relating the relaxation strength, β_r/β_o, and the ΔH, ΔV for a chemical reaction can be obtained in two ways. The first and most common is making use of irreversible thermodynamics. The second approach was introduced by Andreae in 1964 and simply compares expressions for compressibility, heat capacity and expansion coefficient. Whether the derivation is done by the first or the second method, the final relationship must be the same for the same chemical reaction.

If we now choose a chemical reaction specified by the stoichiometric formula

$$\Sigma\nu_i M_i = 0 \qquad (2.D.24)$$

where ν_i is the stoichiometric coefficient of ith species M_i. In this case the change in mole numbers of the ith constituent due to the reaction is given by

$$dN_i = \nu_i d\zeta \qquad (2.D.25)$$

where ζ is the degree of the reaction and N_i is the number of ith species.

As it is shown in Appendix A, the relation between the relaxation strength and thermodynamic parameters of the reaction represented by 2.D.24 is given by

$$\beta_r/\beta_o = \frac{(\gamma - 1)\delta C_P}{C_{P\infty}} \left[1 - \frac{\Delta V}{\Delta H} \frac{C_P}{V\theta}\right]^2 \qquad (2.D.26)$$

where $\gamma = C_P/C_V$

C_P = heat capacity at constant pressure

C_V = heat capacity at constant volume

$C_{P\infty}$ = heat capacity at constant pressure at very high frequency

δC_P = excess heat capacity due to the relaxation process

ΔV = the volume change of the reaction

ΔH = the enthalpy change

V = the partial molal volume

θ = the expansion coefficient

Furthermore, equation 2.D.26 can be written in the form

$$\beta_r/\beta_o = \frac{+(\gamma - 1)\Delta H^2}{C_{P\infty} T \sum_i \sum_j \nu_i \nu_j [\partial \mu_i/\partial N_j]_{P,T}} \left[1 - \frac{\Delta V}{\Delta H} \cdot \frac{C_P}{V\theta}\right]^2 \qquad (2.D.27)$$

$$\beta_r/\beta_o = \frac{\gamma - 1}{TC_{P\infty} \sum_i \sum_j \nu_i \nu_j (\partial \mu_i/\partial N_j)_{P,T}} \left[\Delta H - \frac{C_P \Delta V^2}{V\theta}\right] \qquad (2.D.28)$$

where μ_i is the chemical potential.

Substituting for β_r/β_o from 2.D.28 into 2.D.22, we get

$$\alpha'/f^2 = \frac{2\pi^2(\gamma - 1)}{vTC_{P\infty} \sum_i \sum_j \nu_i \nu_j (\partial \mu_i/\partial N_j)_{P,T}} \left(\Delta H - \frac{C_P \Delta V}{V\theta}\right)^2 \frac{\tau}{1 + \omega^2\tau^2}$$

(2.D.29)

But $\tau = 1/2\pi f_c$ where f_c is the relaxation frequency.

$$\alpha'/f^2 = \frac{\pi(\gamma - 1)}{vTC_{P\infty}f_c \sum_i \sum_j \nu_i \nu_j (\partial\mu_i/\partial N_j)_{P,T}} \left(\Delta H - \frac{C_P \Delta V}{V\theta}\right)^2 \frac{1}{1 + \omega^2\tau^2} \qquad (2.D.30)$$

2.D.30 can be rewritten as

$$\alpha/f^2 = \frac{A}{1 + (f/f_c)^2} + B \qquad (2.D.31)$$

where $$A = \frac{\pi(\gamma - 1)}{vTC_{P\infty}f_c \sum_i \sum_j \nu_i \nu_j (\partial\mu_i/\partial N_j)_{P,T}} \left(\Delta H - \frac{C_P \Delta V}{V\theta}\right)^2$$

f_c = relaxation frequency

B = the absorption due to the background

and $\sum_i \sum_j \nu_i \nu_j (\partial\mu_i/\partial N_j)_{P,T}$ can be calculated once the stoichiometric equation is known.

E. Multi-step Process

As shown in the preceding section the sound absorption caused by the relaxation of a single reaction is described by equation 2.D.31. If, however, several relaxation times are involved due to a multi-step process, the ultrasonic absorption equation becomes a sum of 2.D.31.

$$\alpha/f^2 = \sum_{i=1}^{i=n} \frac{A_i}{1 + (f/f_{c_i})} + B \qquad (2.E.1)$$

where A_i is the amplitude of ith step and n is the number of the steps causing relaxations.

F. The Cause for the Absorption of Sound Wave in a Fluid

When a sound wave propagates in a liquid where there is no relaxation process taking place, there will be an absorption of the sound wave by the liquid. This type of absorption is commonly called the classical absorption and was originally derived by Stokes. As a result of the vibration of the waves in the liquid, the particles of the medium are displaced relative to their position of rest; consequently, internal friction forces exist and absorption of sound occurs. According to Stokes the absorption coefficient, α, in a liquid is proportional to the ordinary, or shear, viscosity and the square of the frequency.

$$\alpha = 2\eta f^2/3\rho v^3 \qquad (2.F.1)$$

where η is the shear viscosity

ρ is the density of the liquid

v is the velocity of the wave

Kirchhoff pointed out that an additional term due to the thermal conductivity of the medium should be considered in some cases. Litovitz has shown that a modified combination of both viscosity and thermal conductivity give rise to the absorption.

$$\alpha = \frac{2\pi^2}{\rho v^3}\left[\frac{4}{3}\eta + (\gamma - 1)\, K/C_P\right] \cdot f^2 \qquad (2.F.2)$$

where K is the thermal conductivity of the medium.

When the sound waves vibrate in a liquid or solution where there is chemical relaxation, an excess absorption is observed plus the classical type. This will depend on how rapidly the equilibrium state is established compared to the period of the oscillation of the wave.

Suppose the equilibrium causing the relaxation is too slow or too

fast compared to the period of oscillation of the wave. In these two cases no excess absorption per wavelength will take place since in the first case the extent of the reaction remains practically unaffected (Fig. 2, curve a), while in the second case it will follow very closely the variation of the sound wave (curve b, Fig. 2).

In the case where the relaxation time of the equilibrium is comparable with the time period of the wave, the extent of the reaction lags behind the wave and therefore a phase difference takes place. Such phase difference leads to dissipation of mechanical energy as heat and so to absorption of power from the wave. The excess absorption will go through a maximum as the frequency increases, shown mathematically in Section D, at a frequency given by $\omega\tau = 1$.

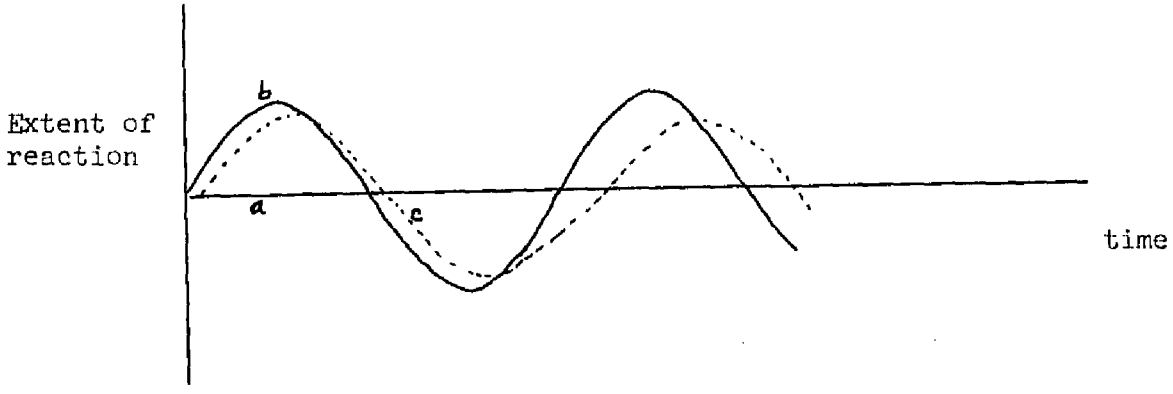

Fig. 2. Periodic perturbation of chemical equilibrium by external parameter.

CHAPTER III

EQUIPMENT AND EXPERIMENTAL PROCEDURE

This chapter deals with the description of the ultrasonic equipment used in the experimental studies, the preparation of the solutions and the procedure for obtaining the experimental data.

A. Ultrasonic Equipment

Figure 4 shows a block diagram of the ultrasonic apparatus used in the present work. The pulse technique has been used in the measurements. The apparatus consists of four major units: (1) the ultrasonic cell, (2) ultrasonic attenuation comparator,* (3) signal generator** and (4) frequency meter.***

1. Ultrasonic cell.

The cell consists of two main parts (Fig. 3). The lower part is made of a 100 cc stainless steel container holding at its bottom a 1-in. receiving crystal transducer. The top plate of that container has a 1.5" diameter machined hole. The upper part of the cell contains a stainless steel head holding a 1/2" transmitting crystal and a 1-in long fused quartz delay line. This holder is driven by a micrometer that has a 5-cm total path length and can show path changes within $\pm$ 1.0 x 10^{-4} cm. Both the transmitting and the receiving crystals[35] are X-cut quartz with the same thickness in order to have the same fundamental frequency. They

*Ultrasonic attenuation comparator is a Matec Model PR-201.
**Signal generator is Hewlett-Packard 608D VHF Signal Generator.
***Frequency meter is Gertsch (Model FM-3).

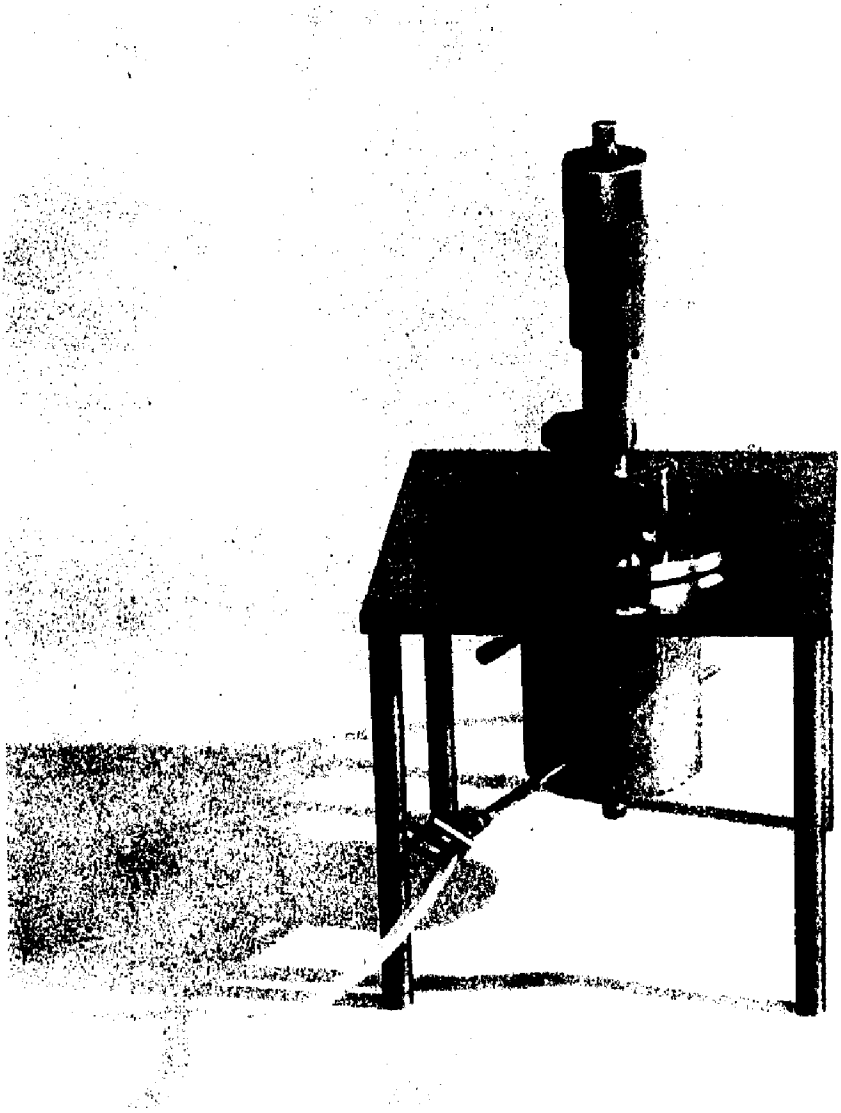

Fig. 3a. Ultrasonic Cell

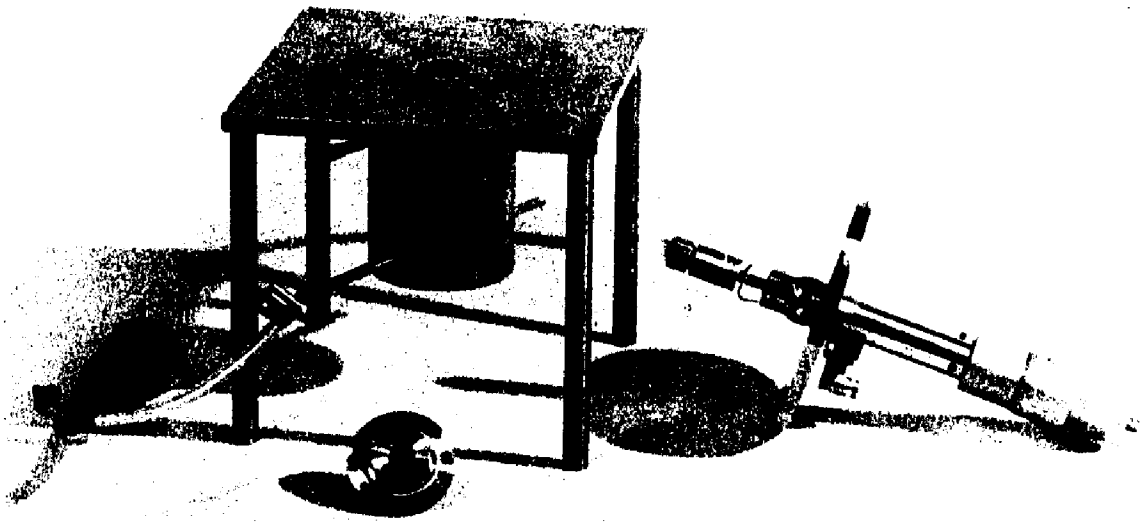

Fig. 3b. Components of Ultrasonic Cell

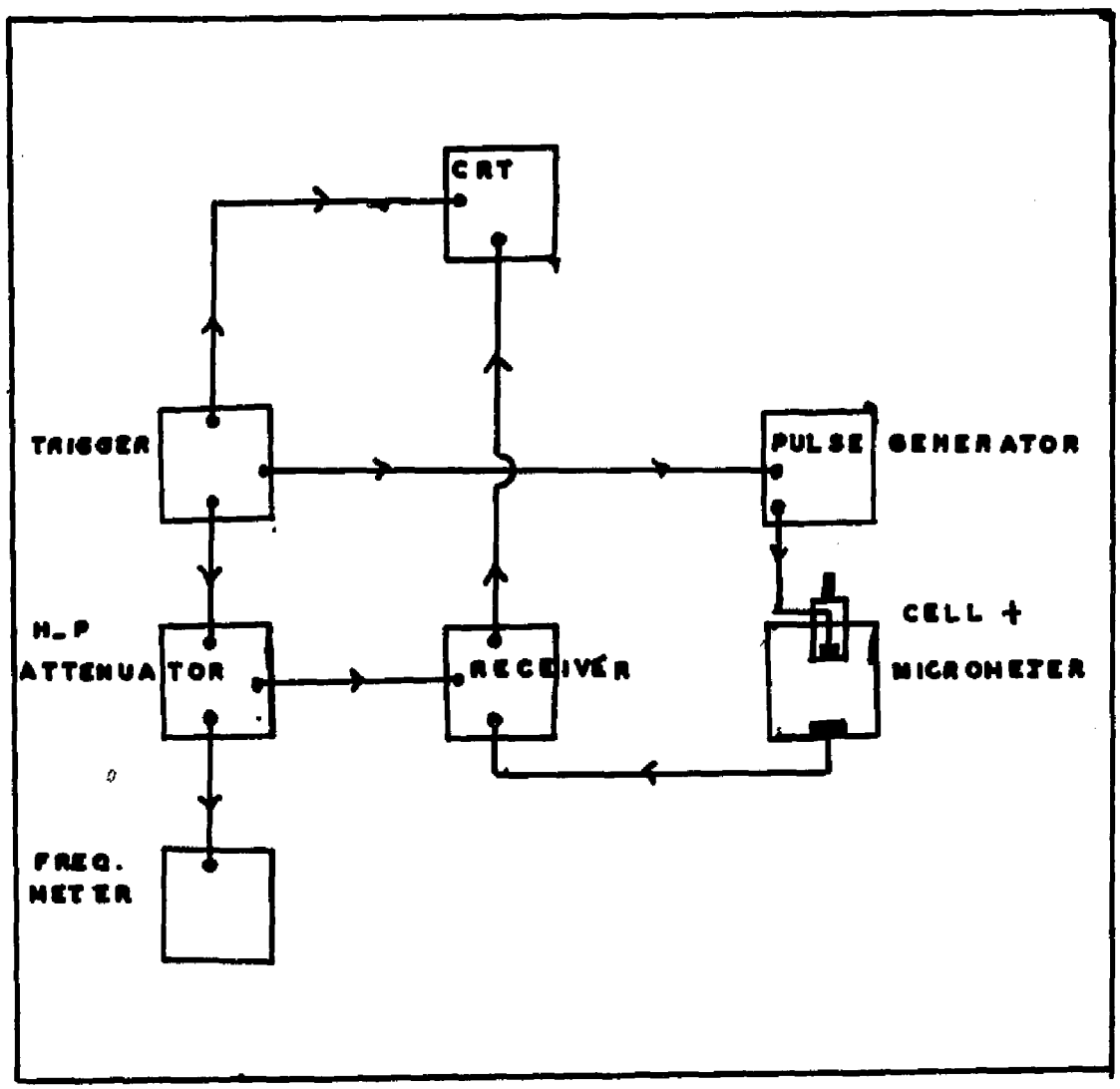

FIG. 4

BLOCK-DIAGRAM OF ULTRASONIC APPARATUS

were gold plated for electrical contact. Maximum acoustic energies are obtained by operating at the fundamental natural frequencies, but for the propagation of the high frequencies, used in the present study, it was necessary to use upper harmonics. The delay line in contact with the 1/2" crystal prevented electrical cross-talk between receiver and transducer crystals.

The cell container has double walls through which water is circulated from a thermostated bath at the desired temperature.

When the upper and lower parts of the cell are held together, they are very well sealed and no air can get in.

2. Ultrasonic attenuation comparator.

It consists of most of the electronic system for performing the operations required in making measurements of ultrasonic attenuation in the solutions under investigation. The following are its major constituents:

(a) pulsed oscillator, with frequency range 1-200 Mc/sec, which operates at a repetition rate of 100 pps with pulse widths of .5, 1 and 2 μsec.

(b) high gain superheterodyne receiver, of frequency range 5-200 Mc/sec.

(c) all necessary oscilloscope functions including a built-in 5" CRT.

(d) synchronizing circuits to provide dual display.

(e) a trigger circuit with basic repetition-rate of 200 pps.

3. Signal generator.

Model 608D VHF signal generator furnishes rf signals from .1 microvolt to .5 volt over the frequency range 10 to 420 MHz. The level of the output signal is regulated by an attenuator which is adjusted by a

calibrated front-panel control. The attenuator is calibrated in both volts and decibels and can be read directly to an accuracy of ± 1 decibel over the full frequency range.

4. Frequency meter.

It is used to accurately measure the frequency at which the absorption measurement is made. The FM-3 type is a heterodyne frequency meter in which frequencies are measured by heterodyning two signals together in a detector and adjusting them for zero difference as indicated by the difference frequency heterodyne beat note.

B. Chemicals and Solutions

Cyclohexane: Fresh 500 ml bottles of spectroquality reagent purchased from Matheson Coleman and Bell Company. It was distilled from P_2O_5 and then kept over molecular sieves.

ε-caprolactam: (2-oxohexamethylenimine) from Matheson Coleman and Bell Company. Vacuum distillation was carried out and the collected material was kept in a vacuum dessicator over Dririte.

Carbon tetrachloride: Spectroquality reagent from Matheson Coleman and Bell Company. It was used as received with no further purification.

Toluene: Fisher certified A.C.S. grade, used with no further purification.

Dioxane: Fisher certified, used with no further purification.

Water: Triply distilled.

Preparing solutions. Care was taken while preparing the solutions for the measurements, to prevent exposure to the air. To achieve this the whole process of preparation, including weighing the samples themselves, was done inside a dry box. All the glass used was first dried in an oven, and then flushed several times with dry nitrogen.

C. Experimental Procedure

The cell container was cleaned thoroughly and purged with a stream of dry nitrogen for a half hour before inserting the solution to be measured. About 50 cc of solution was needed for each run. The upper part of the cell is adjusted by means of three screws on the top plate of the lower part to make sure of the parallelism between the receiving and transmitting crystals. The pulsed oscillator generates short bursts of radiofrequency energy, of desired frequency, which are converted to mechanical energy, ultrasound, by means of the transmitting crystal. When the sound pulse waves travel in the solution, it is attenuated. Each pulse will generate a small amount of electrical energy at the receiving transducer. This energy is coupled to the high gain receiver where it is amplified, detected and then displayed on the oscilloscope screen. However, at the receiver only a fraction of the pulse is converted; most is reflected. Since the sound pulses in passing back and forth through the solution will continuously lose energy, the echoes as displayed on the oscilloscope will eventually decay out. The rate of decay is characteristically exponential.

Attentuation measurements are made by comparing the change in height of the first cell signal with an equal change in height of the pulse produced by the signal generator which is amplified through the same receiver used for amplification of the signal coming out of the cell.* The height of the comparator signal was varied and accurately read and the signal from the cell was made to match the same height by varying the

---

*The pulser, signal generator and receiver were tuned to the same frequency. To accomplish this at higher frequencies a Weinschel DS-109H double-stub tuner between the oscillator and the transmitting crystal is used.

distance between the two crystals. The absorption coefficient, α, is simply determined by reporting, at the same frequency, the variation of distance with attenuation. The slope of the straight line of attenuation, in db, versus distance, in cm, was taken as α in db cm^{-1}. The details of obtaining the absorption coefficient from the measured data are explained in the next chapter.

CHAPTER IV

EXPERIMENTAL RESULTS AND DATA ANALYSIS

Ultrasonic absorption measurements were carried out in ε-caprolactam-solvent solutions as a function of four different parameters. The measurements were initially made in five solvents at 25°C. The excess absorption in the solutions of four of these solvents, toluene, dioxane, water and CCl_4 was small and the change with frequency was negligible. In cyclohexane as a solvent a measurable excess absorption is observed. In the latter case data were obtained at four different temperatures and three different concentrations at each temperature. For each concentration the absorption coefficient, α, was determined at different frequencies in the range 10-130 MHz. The limitations for wide range measurements in each parameter is discussed. The analysis of raw data, namely, attenuation versus distance, used to obtain α, is explained. The variation of α with frequency is used to determine the various relaxation parameters for a single relaxation equation.

A. Evaluation of Absorption Coefficient, α, from Raw Data

The absorption coefficient, α, defined earlier in Chapter II, is given by the following equation,

$$I = I_o \exp(-2\alpha X)$$

where I and I_o are the sound intensity at distances X and X = 0.

What we actually are measuring is the attenuation in decibels* as a

*1 db = $10 \log_{10} I/I_o$.

function of the distance between the two crystals. The slope of a plot attenuation versus distance yields the absorption of the solution in terms of decibels cm^{-1}. This value is then converted to the pressure amplitude absorption coefficient which has units of neper* cm^{-1}. The only advantage of expressing α in terms of neper cm^{-1} is that most of the ultrasonic data are reported in this form in the literature. A computer program (see Appendix B2) was written and used to evaluate the slope of each attenuation-distance set by means of a least squares technique (see Appendix B1). The results of three or four such series at the same frequency were obtained and averaged for each value of α. The same program was also designed to calculate the standard deviation (Appendix B1) in α at each frequency.

To assure that there is no relaxation occurring in the pure solvents their absorption coefficients were measured. Indeed the values of α/f^2 in all solvents are found to be constant in the frequency range 10-130 MHz. These results are shown in Tables XI and XII in Appendix D.

B. Effect of Concentration

When the temperature is kept constant and measurements are made at various concentrations, in the range .026 M^{-1} to .15 M^{-1}, a noticeable change in the α/f^2 values is observed. It would have been more favorable to work with a much wider concentration range. Unfortunately, this is not possible because, at lower concentrations ($< .01\ M^{-1}$) the excess absorption becomes too small; and at higher concentrations ($> .18\ M^{-1}$) the solubility becomes a barrier.

---

* 1 neper = 8.686 db.

C. Effect of Temperature

The absorption was measured at four temperatures, 6, 10, 17 and 25°C for the ε-caprolactam-cyclohexane solutions. The values of α/f^2 for the same concentration and the same frequency showed, at most frequencies, an increase as the temperature was decreased. Measurements could not be made at temperatures below 5°C because of freezing problems nor higher than 30°C due to decrease in α/f^2 values with temperature.

D. Effect of Frequency

In all the concentrations at the various temperatures the absorption coefficient is measured as a function of frequency in the range 10 to 130 MHz. From this change a fitting type procedure is carried out, as will be shown later, and a single relaxation fit is obtained.

The results showing the above three effects (B, C and D) are tabulated, see Appendix D, in Tables XIII through XXIV. The same results are plotted (α/f^2 vs log f) in Figs. 5, 6, 7 and 8. The solid lines are the theoretical values and the points are the experimental ones.

E. Evaluation of Relaxation Parameters A, f_c and B

These three parameters are determined by a fitting of the theoretical single relaxation equation, by least squares method,

$$\alpha/f^2 = \frac{A}{1 + (f/f_c)^2} + B \qquad 2.D.31$$

to the experimental data, $(\alpha/f^2)_{exp}$. The detailed procedure is fully explained in Appendix C1. A computer program is used to evaluate these parameters (see Appendix C2). The results are shown in Table II.

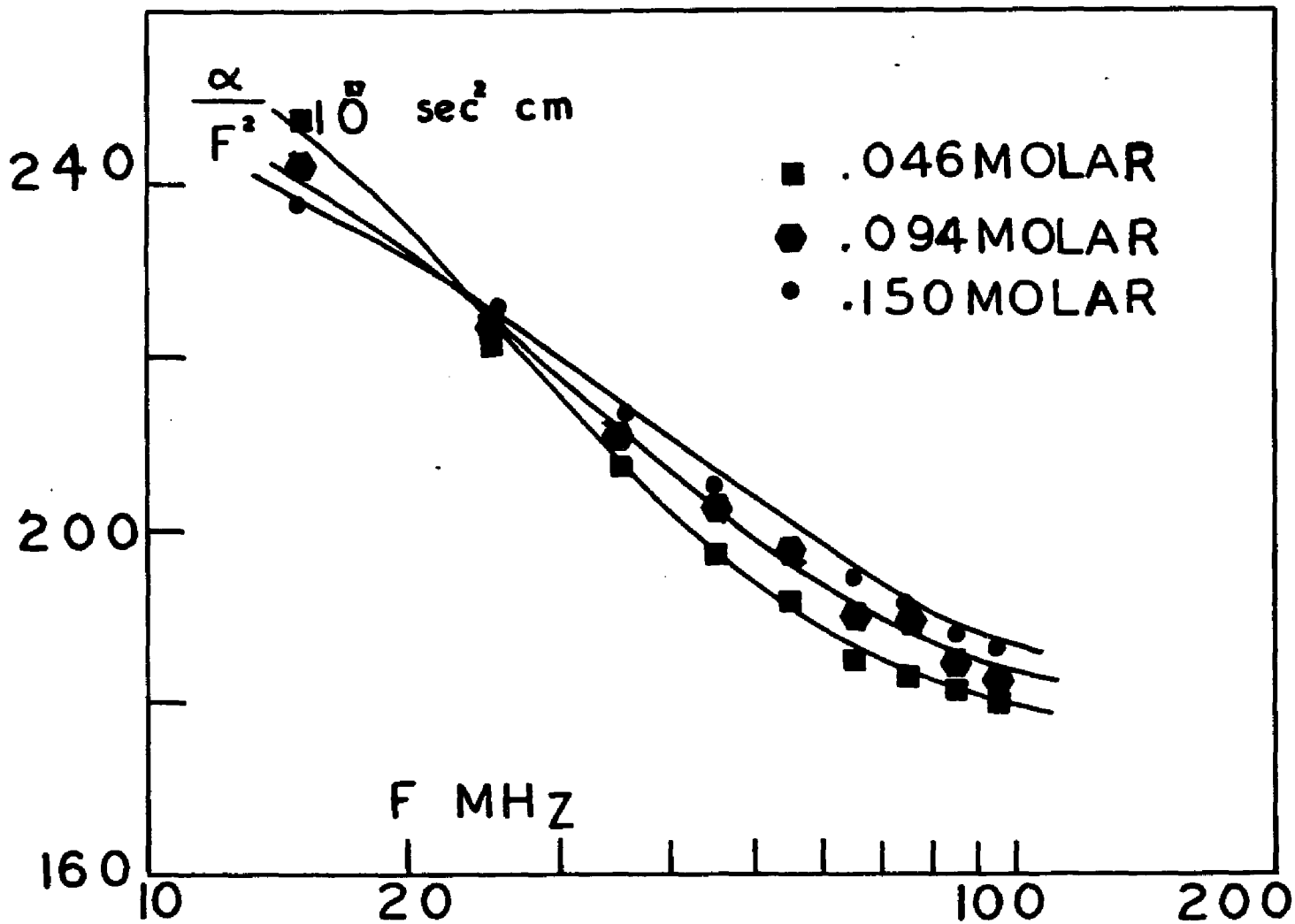

FIG. 5 $\frac{\alpha}{F^2}$ VS. LOG. F OF ϵ-CAPROLACTAM IN CYCLOHEXANE, 6°C

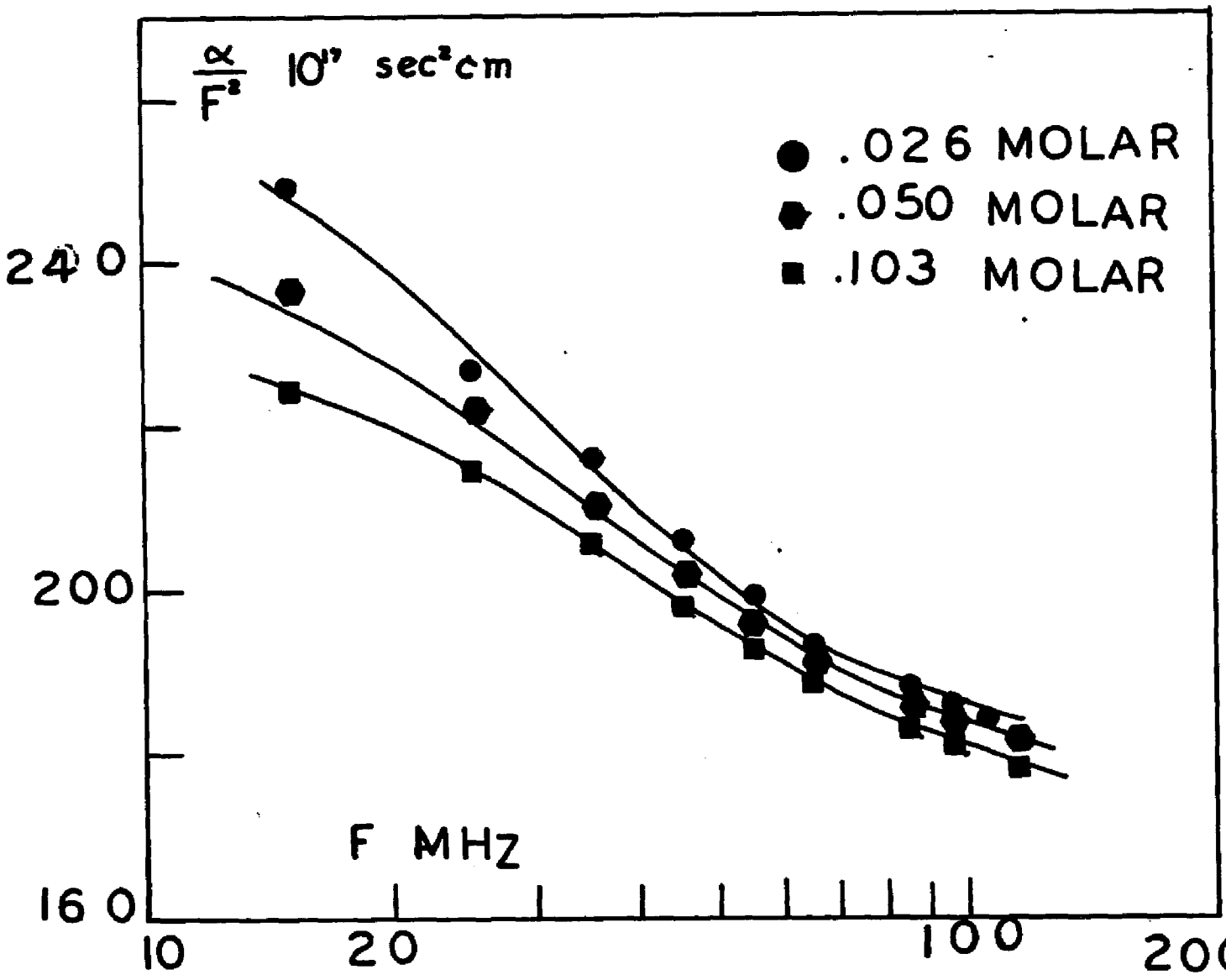

FIG. 6 $\frac{\alpha}{F^2}$ VS. LOG. F OF ϵ-CAPROLACTAM IN CYCLOHANE, 10°C

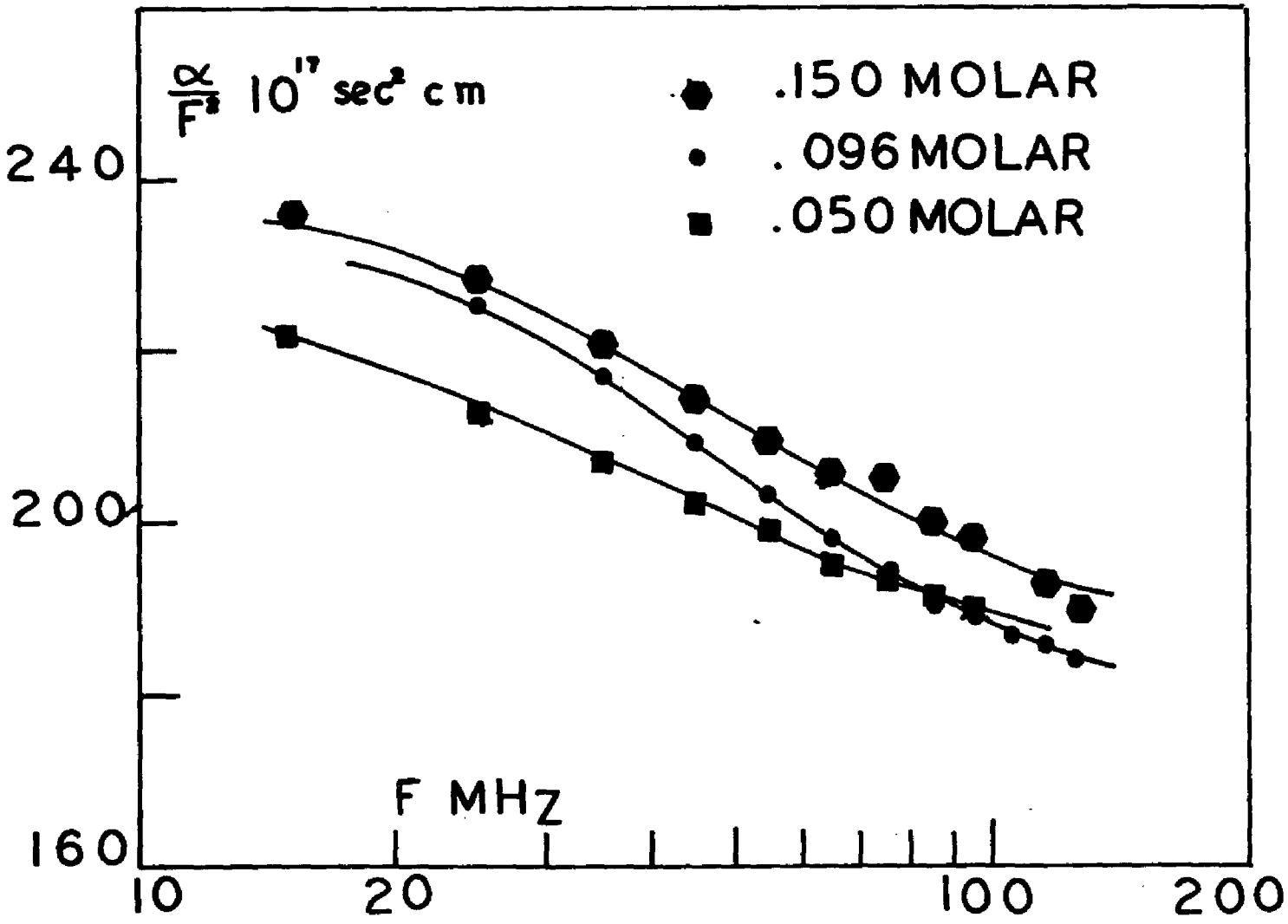

FIG. 7 $\frac{\alpha}{F^2}$ VS. LOG. F OF ϵ-CAPROLACTAM IN CYCLOHEXANE, 17°C

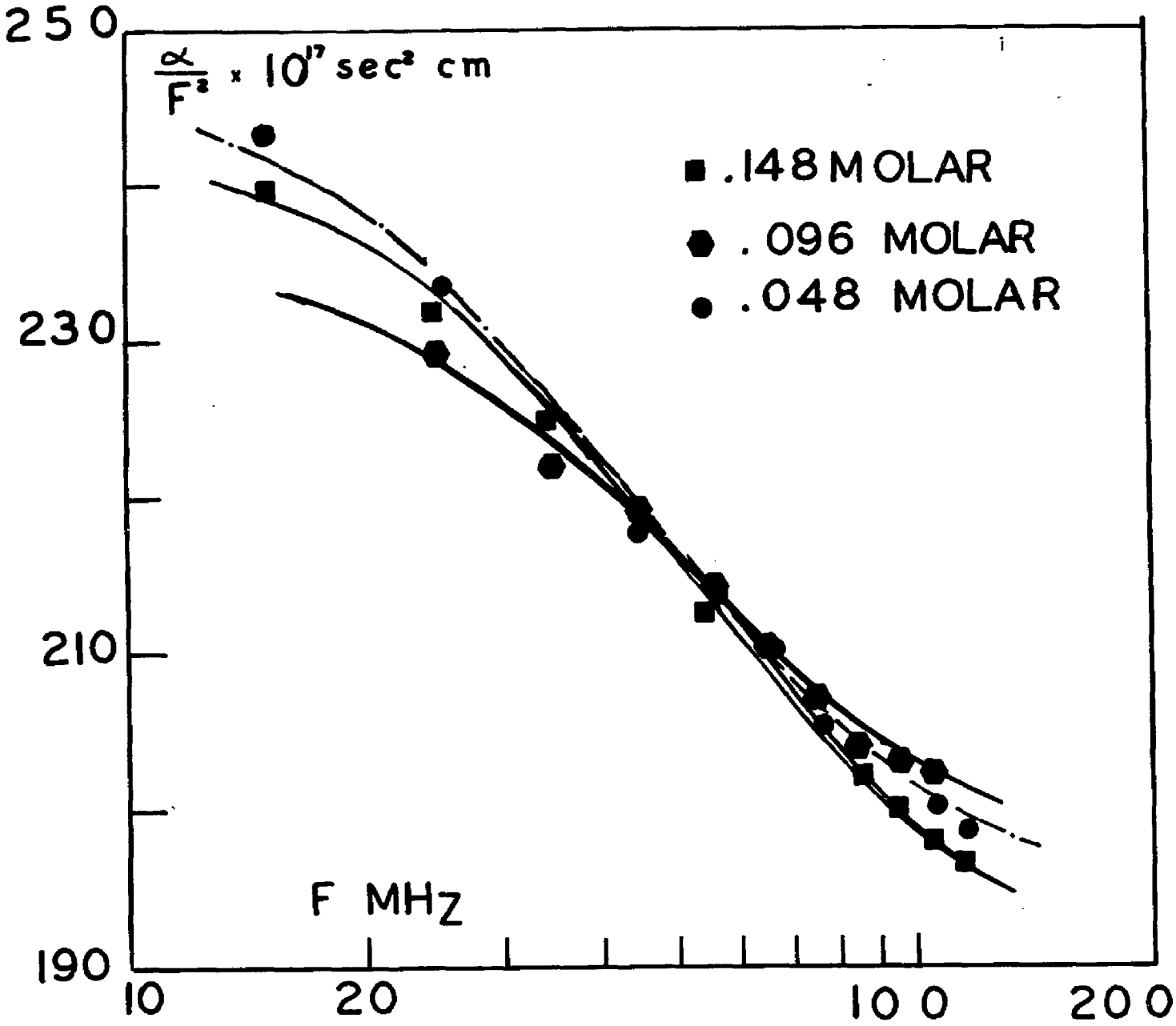

FIG. 8 $\frac{\alpha}{F^2}$ VS. LOG. F OF ϵ-CAPROLACTAM IN CYCLOHEXANE, 25°C

Table II. Values of the Relaxation Parameters

Temp °C	Conc. Molar	f_c MHz	τ^{-1} 10^{-6} x sec^{-1}	A sec^2 cm	B sec^2 cm
6	.046	26.79 ± 1.71	168.2 ± 10.7	95.1 ± 3.4	172.5 ± 1.4
	.0943	33.32 ± 2.14	209.3 ± 13.4	79.5 ± 2.3	175.1 ± 1.7
	.150	35.77 ± 1.12	224.6 ± 7.0	75.2 ± 1.0	177.1 ± 1.0
10	.0256	31.30 ± 1.79	196.6 ± 11.2	80.1 ± 4.1	178.7 ± 2.4
	.050	35.51 ± .65	223.0 ± 4.1	69.2 ± 1.0	175.4 ± 1.0
	.103	39.68 ± 1.04	249.2 ± 6.5	62.2 ± 1.0	172.9 ± 1.0
17	.050	42.02 ± 3.40	263.9 ± 21.4	38.8 ± 2.0	183.3 ± 2.1
	.096	47.70 ± 2.84	299.9 ± 17.9	62.1 ± 1.7	176.8 ± 1.2
	.150	50.96 ± 4.80	320.0 ± 30.1	52.6 ± 2.9	184.3 ± 3.2
25	.048	48.68 ± 5.50	305.7 ± 34.5	53.1 ± 2.4	189.6 ± 2.1
	.096	51.72 ± 7.10	324.8 ± 44.6	50.1 ± 2.4	192.4 ± 2.5
	.148	54.91 ± 5.52	344.8 ± 34.7	56.5 ± 2.4	185.5 ± 2.6

F. Calculation of the Relaxation Time

Having evaluated the relaxation frequency, f_c, from the fitting procedure the calculation of the relaxation time is then very straightforward. It is calculated by use of the following equation:

$$\tau = 1/2\pi f_c \quad .$$

The results of the relaxation times are also tabulated in Table II.

CHAPTER V

MODELS

An acceptable model used to interpret kinetic data in terms of a physical or chemical process must have the following characteristics:

a. be the simplest mechanism possible which describes the process (and fulfill the following conditions),

b. be able to describe the experimental data, and

c. be consistent with other results, e.g., rate constants, equilibrium constants, obtained by other workers on similar systems.

In this chapter the models suggested previously by several authors on similar systems are considered. These models include monomer-dimer (one-step reaction), monomer-tetramer (one-step reaction), and monomer-dimer (two-step reaction). Two models are used to interpret the data obtained on the present system. These are the monomer-dimer through one and two steps. The former is ruled out for reasons which are discussed later.

A. Previous Models Suggested in the Literature for Similar Systems

1. Monomer-dimer (one-step reaction).

Monomers of acetic acid,[14] benzoic acid[15] and some others in organic solvents are thought to form their corresponding dimers through a one-step process. Also, 2-pyridone[22] in different solvents was assumed to follow this type of mechanism. This can be represented by

$$2A \underset{k_b}{\overset{k_f}{\rightleftharpoons}} A_2 \qquad (5.1)$$

where A is the monomer and A_2 is the dimer, k_f and k_b are the forward and reverse rate constants. The association constant of the dimerization is given by

$$K_A = \frac{k_f}{k_b} = \frac{[\bar{A}_2]}{[\bar{A}]^2} \qquad (5.2$$

where $[\bar{A}_2]$ is the equilibrium dimer concentration

$[\bar{A}]$ is the equilibrium monomer concentration.

If we now follow the same procedure as in Chapter II.C., the following relationship between the relaxation time and the rate constants is given by

$$1/\tau = 4k_f[\bar{A}] + k_b \qquad (5.3)$$

Assuming that monomers and dimers are the predominant species present, then

$$A_o = [A] + 2[A_2] \qquad (5.4)$$

where A_o is the stoichiometric concentration. Substituting 5.2 into 5.4 and solving for $[\bar{A}]$ we obtain

$$[\bar{A}] = -\frac{k_b}{4k_f} + \frac{k_b\sqrt{1 + 8K_A A_o}}{4k_f} \qquad (5.5)$$

Substituting for $[\bar{A}]$ into 5.3 and squaring both sides of the equation, we obtain

$$1/\tau^2 = 8k_f k_b A_o + k_b^2 \qquad (5.6)$$

Experimentally, the relaxation time is evaluated at several stoichiometric concentrations of the solute. Then, the first step in examining the validity of the model represented by 5.1 can be done by plotting $1/\tau^2$ versus A_0. A straight line should be obtained, the slope and the intercept of which must be positive. The forward and reverse rate constants can then be evaluated. 2-pyridone in p-dioxane seems to follow the above mechanism but when 2-pyridone in equal amounts of p-dioxane-CCl_4 mixture was tested for equation 5.6, a straight line was obtained only at high concentration. A curvature appeared at lower concentrations. The authors attributed such curvature to non-ideality. This does not seem to be a satisfactory explanation, because non-ideality should cause at least as much curvature at high concentration as at lower. Another argument, originated by Rassing, asks why non-ideality should appear in the CCl_4-p-dioxane mixture and not in the case of pure p-dioxane. Most cases of simple H-bonded solutes in nonaqueous solvents studied so far and explained on the basis of this model have also been explained by other authors on the basis of either formation of higher polymers, or two-step dimerization.

2. Monomer-tetramer (one-step mechanism).

There is only one case where such a model is considered. This case is the original explanation of the single relaxation observed in the t-butanol-cyclohexane[18] system. This model can be represented as

$$4A \underset{k'_{21}}{\overset{k'_{12}}{\rightleftharpoons}} A_4 \quad , \tag{5.7}$$

where A is the monomer and A_4 is the tetramer. k'_{12} and k'_{21} are the forward and reverse rate constants.

When the same procedure as in II.C. is done, we get the following relaxation expression:

$$1/\tau = 16k_{12}[\bar{A}]^3 + k_{21} . \qquad (5.8)$$

It is clear that a plot of $1/\tau$ versus $[\bar{A}]^3$ must yield a straight line of positive slope and intercept. Although the authors concluded, in the above case, that 5.7 is the best model to explain their experimental data, they also mentioned that their data did fit two other models. These are monomer-dimer through one step and monomer-trimer through one step. They, however, ruled out the former, because it gave a negative intercept and the latter because the trimer concentration calculated from the experimental equilibrium constants was greater than could be formed from all the available alcohol molecules. However, it seems that a negative intercept may be an indication of the monomer-dimer formation in two steps proposed by Rassing.

3. Monomer-dimer (two-step mechanism).

This model assumes the rupture of the two hydrogen bonds of the dimer in solution in a stepwise fashion, each step with its characteristic relaxation time. Tabuchi[36] was the first to consider the two-step model for the case of pure acetic acid using Lamb and Pinkerton's[37] ultrasonic data. Recently Rassing used this model to interpret Hammes' data on 2-pyridone in organic solvents with some success. The ultrasonic data of the system under investigation also fit this mechanism. The two-step mechanism is represented by

$$2A \underset{k_{21}}{\overset{k_{12}}{\rightleftharpoons}} A\cdots A \underset{k_{32}}{\overset{k_{23}}{\rightleftharpoons}} A\cdots A$$

(1) (2) (3)

and its mathematical treatment was done in Chapter II. Tabuchi assumed that the observed single relaxation (having a relaxation frequency in the range 0.5 to 4 Mc/sec in the temperature range 20-60°C) is due to the perturbation of the equilibrium of the second step. Rassing, however, assumed that the two steps have very close relaxation times and one can only obtain a mean value of the relaxation time. He related this relaxation time to all the constants involved in the two steps.

We feel that in order to consider the validity of the Rassing model one should have first fitted his data to the one-step model and proved (with strong evidence) the nonvalidity of such model. An important point must be made here: that to further examine the Rassing approach for the two-step model a wide range of concentrations must be studied. Eigen, Bergmann and de Maeyer assumed the possibility of the two-step model when they studied the dielectric relaxation of ε-caprolactam in CCl_4 and in benzene solutions. They could only, however, calculate apparent forward and backward rate constants of the overall process. This is due to the fact that they can only study the overall mechanism using their technique, unless there is a great change in the dipole moments of the initial and the final states of each step. In addition, their measurements were only carried out at one temperature, 22°C.

In the next section this model, as well as the one-step model, are considered for the system under investigation.

B. Proposed Models on the System under Investigation

Introduction.

From spectroscopic studies of ε-caprolactam in CCl_4 and other organic solvents there is evidence supporting the presence of monomers and dimers. There is also some evidence of the possibility of having

both types of dimers, open and cyclic, in the concentration range used in this work.

Two models are considered, dimerization through one and dimerization through two steps, for interpreting the experimental data obtained through the ultrasonic measurements on ε-caprolactam-cyclohexane solutions. Both of the two mechanisms fit the experimental data within the predicted experimental errors. The equilibrium constants, obtained from the one-step mechanism at all temperatures studied, are far less than the one available from the spectroscopic technique (ε-caprolactam in CCl_4). It is believed, then, that the second mechanism, namely, the formation of the dimer through two steps, is the correct model.

One-step Model.

When we consider the formation of the cyclic dimer in one step (5.1), eq 5.6 is used and τ^{-2} is plotted versus A_o (Fig. 9). Straight lines are obtained at the four temperatures. From the slope and the intercept of each line k_b and k_f are determined at all temperatures. These rate constants and the corresponding equilibrium constant (K_A) are reported in Table III. The errors estimated for the forward rate constants are in the order of 15-25% of their values. For this reason their change with temperature (except at 25°C where errors are higher as seen in Table II) can be considered small. However, the trend of k_f to decrease with increasing temperature is very suspect.

The equilibrium constants of monomer association of ε-caprolactam in cyclohexane and in CCl_4 can be assumed to be similar. This is a fair assumption considering that these two solvents are inert and have very similar dielectric constants and viscosities. We can then compare the values of equilibrium constants (K_A) in Table III to those calculated

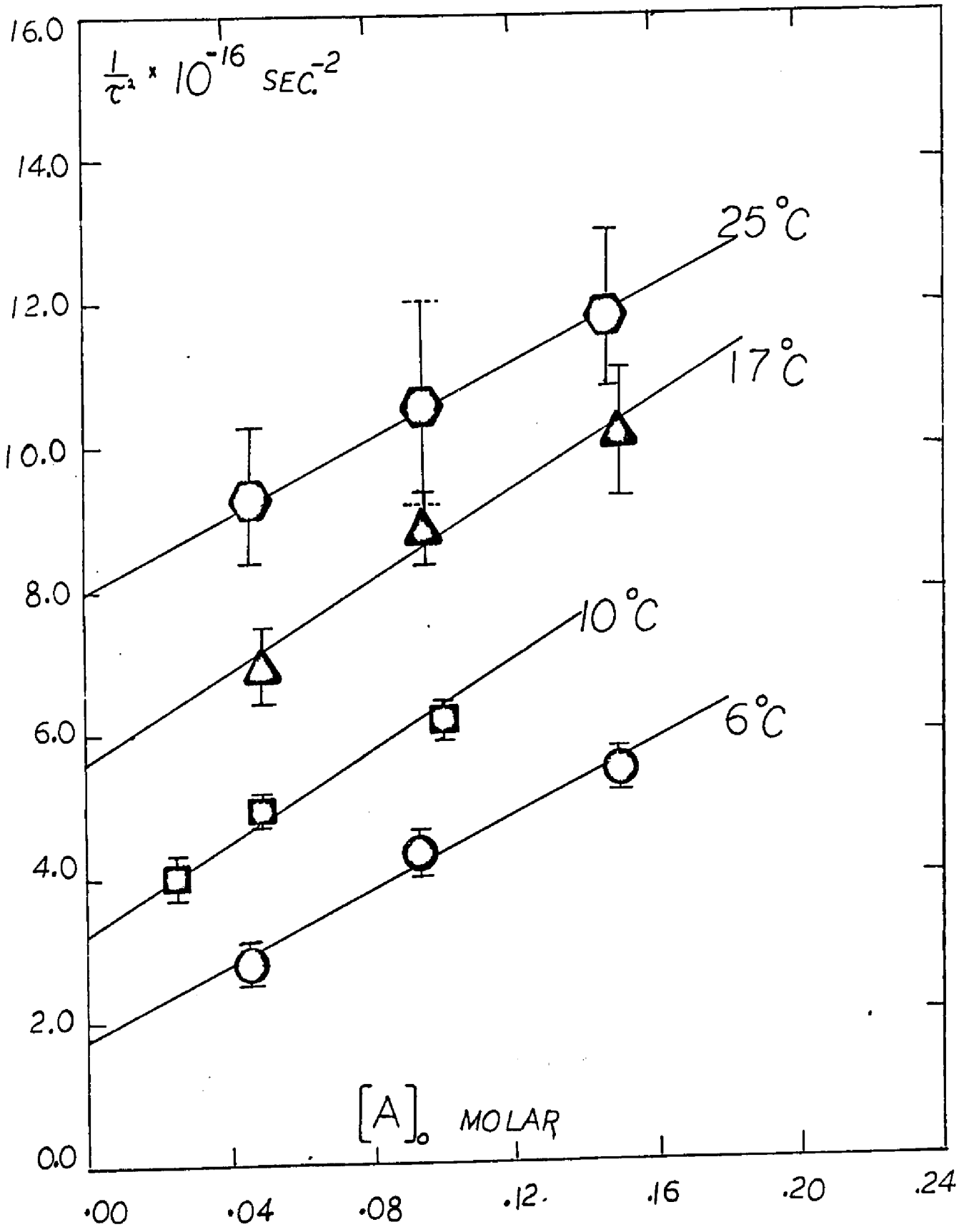

FIG. 9 τ^{-2} VS. CONC. OF ϵ-CAPROLACTAM IN CYCLOHEXANE

Table III. Rate Constants and Equilibrium Constants for One-step Model

Temp	k_f	k_b	K_A	K_{IR}
°C	10^{-8} l M^{-1} sec^{-1}	10^{-8} sec^{-1}	l M^{-1}	l M^{-1}
6	2.43	1.34	1.81	204
10	2.16	1.79	1.21	181
17	1.58	2.37	.67	141
25	1.15	2.83	.41	114

by interpolation from the spectroscopic data by Lord and Porro (K_{IR}) in Table III. Figure 10 shows the ln K_{IR} versus 1/T using their IR data. The calculated values, K_A, using the one-step model are smaller by at least two orders of magnitude than those calculated by Lord and Porro using the same model. This difference is clearly beyond the experimental errors in either case. This then suggests that we are not looking at the same mechanism. We feel that although this model is the simplest model to fit the experimental data, it cannot be the correct one. We then consider the next simplest model, that in which the dimer is formed in two steps.

Two-step Model.

In dealing with this model two cases have been discussed in the theoretical part of Chapter II. The first case, studied by Rassing, assumes that the relaxation times of the two steps are nearly equal and their ultrasonic absorption amplitudes are close to each other in magnitude. The full mathematical treatment was explained earlier and the final form of the relaxation time is given by

$$1/\tau^2 + U(1/\tau) = VA_o + S \qquad (2.C.32)$$

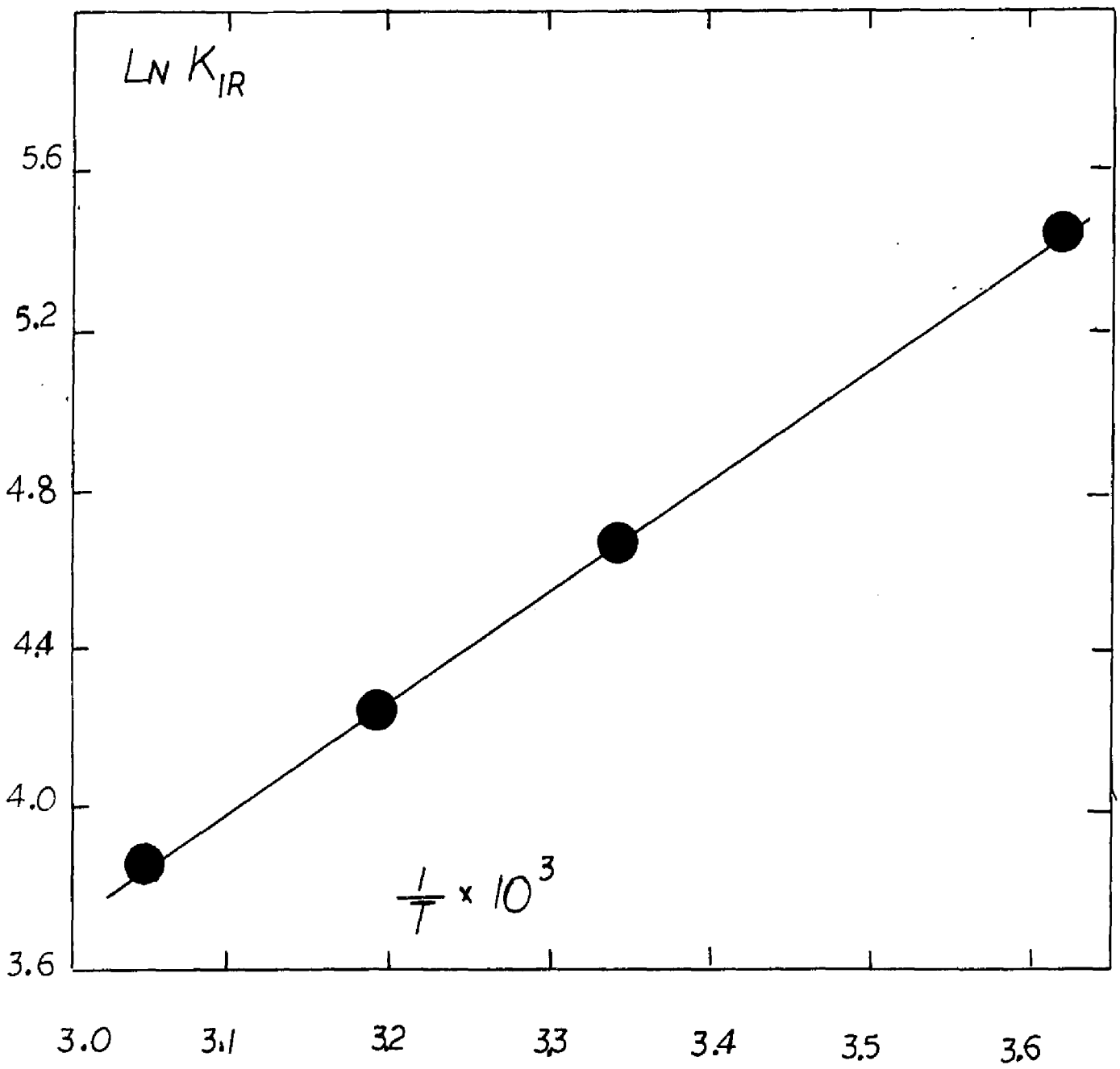

FIG. 10 LN K_{IR} VS. $\frac{1}{T}$ OF ϵ-CAPROLACTAM IN CCL_4

where U, V, S are functions of the rate constants of the two steps and A_o is the stoichiometric concentration. This model is not considered in explaining the data of the present system due to the fact that when $1/\tau^2$ was plotted versus A_o (Fig. 9), no curvature was obtained in the low concentration range and no negative intercepts were observed. However, it should be made clear that the concentration range in our study is not wide enough, due to practical difficulties, to unambiguously decide on the validity of 2.C.32.

The second case of this model is that in which the relaxation times of the two steps (τ_1 and τ_2) are different. Two possible conditions can emerge in this case: the first, in which τ_1 is smaller than τ_2; while the second, that for which τ_1 is larger than τ_2. We have seen from the mathematical derivation in Chapter II that the two relaxation times for the condition $\tau_1 < \tau_2$ can be given by

$$1/\tau_1 = k_{21} + 4k_{12}[\overline{A}] \qquad (2.C.39)$$

and

$$1/\tau_2 = k_{23} + k_{32} - k_{23}\left(\frac{1}{4K_1[\overline{A}] + 1}\right) \qquad (2.C.41)$$

For the other condition ($\tau_1 > \tau_2$), it can be shown, starting from 2.C.16, that the two relaxation times are given by

$$1/\tau_1 = k_{21} + 4k_{12}[\overline{A}] - \left[\frac{k_{21}k_{23}}{k_{23} + k_{32}}\right] \qquad (5.9)$$

and

$$1/\tau_2 = k_{23} + k_{32} \qquad (5.10)$$

Theoretically, two relaxations should be observed for the two-step model, with τ_1 different from τ_2, if a wide frequency range is studied and the ultrasonic amplitudes of the two steps are of reasonable size. We only observe one relaxation process in the frequency range (15-125 MHz)

studied. We now need to decide whether this observed relaxation is due to the first step or the second. It would also be useful to answer the question of which step is faster. If the observed relaxation were due to the first step, then it would be difficult from ultrasonic data alone to decide whether the first step is faster or slower than the second step. This is obvious because of the fact that τ_1^{-1} is linearly dependent on $[\overline{A}]$ in both cases (eqs 2.C.39 and 5.9). One can easily notice that the forward rate constant, k_{12}, will be the same whether τ_1 is smaller or larger than τ_2. This can be understood much more easily if this particular step is controlled by the diffusion of the monomer species. The value of k_{21} can be quite different, depending on the value of the equilibrium constant of the second step.

If, however, the observed relaxation were due to the second step, then the ultrasonic results will be able to discriminate between the two conditions. For $\tau_1 < \tau_2$ we observe that τ_2^{-1} is concentration dependent (eq 2.C.41) while in the other case, $\tau_1 > \tau_2$, τ_2^{-1} is concentration independent (eq 5.10). Since the observed relaxation times are concentration dependent (see Table II), we can eliminate the possibility that the observed relaxation is due to the second step when $\tau_1 > \tau_2$.

From the previous discussion we have seen that if the data fits 2.C.39 or 5.9 the forward rate constant, k_{12}, will be the same, while the backward rate constant, k_{21}, could be different. But it is important to note that we cannot easily tell whether τ_1 is smaller or higher than τ_2. Therefore we consider the condition $\tau_1 < \tau_2$ to see whether the observed relaxation is due to the first step (2.C.39) or the second (2.C.41). If it is the second step, then evidence of another relaxation should be observed at higher frequencies. If this were the case, however,

the absorption of the background, B, in eq 2.D.31 should be higher than the pure solvent value. The B values obtained from fitting the theoretical single relaxation eq 2.D.31 to the experimental data (Table II) are equal to the α/f^2 values of the pure solvent to within experimental error (Appendix D). On the other hand, if the ultrasonic absorption amplitude (A) of the first step is quite small compared to that of the second step, then the observed relaxation could still correspond to the second step. Equation 2.C.41 must then fit the experimental relaxation times.

The overall equilibrium constant is taken from the IR data (Table III) to calculate the equilibrium concentration of the monomer (shown in Table IV). Equation 2.C.41 is then fitted by means of a two-parameter fit computer program to the observed relaxation times. Table V shows the fit is good for all the concentrations at all the temperatures.

Table VI shows the rate constants, k_{23} and k_{32}, of the second step with the equilibrium constants of the first (K_1) and second (K_2) step. K_1 and K_2 are related to the overall equilibrium constant, K_{IR}, in the following manner:

$$K_{IR} = K_1(1 + K_2) \qquad (5.11)$$

These rate constants are those values which gave the best agreement between the observed and the experimental relaxation times.

The forward rate constant k_{23} is almost constant within experimental error with increasing temperature. The k_{32} values, however, increase greatly with temperature. The dissociation energy of activation, E_{32}, of the cyclic dimer to open dimer, calculated from the variation of k_{32} with temperature is found to be 11 ± 1 Kcal/mole dimer.

Table IV. Equilibrium Concentrations of Monomer ε-Caprolactam in Cyclohexane

Temp °C	Stoichiometric Concentration $[A]_o$ (moles/liter)	Equilibrium Concentration $10^3 \times [\bar{A}]$ (moles/liter)
6	.046	9.46
	.094	14.00
	.150	19.20
10	.0256	7.04
	.050	10.03
	.103	15.54
17	.05	11.66
	.096	16.76
	.150	21.34
25	.048	12.48
	.096	18.44
	.148	23.38

Table V. Calculated τ_2^{-1} Obtained from the Two-Parameter Computer Program Fit

Temp °C	Concentration M/l	Observed $10^{-8} \times \tau_2^{-1}$	Calculated $10^{-8} \times \tau_2^{-1}$
6	.046	1.68	1.71
	.0943	2.09	2.03
	.150	2.25	2.28
10	.0256	1.96	1.96
	.050	2.23	2.23
	.103	2.49	2.49
17	.050	2.64	2.65
	.096	3.00	2.99
	.150	3.20	3.21
25	.048	3.06	3.04
	.096	3.25	3.29
	.148	3.45	3.42

Table VI. Rate Constants and Equilibrium Constants Obtained from the Two-Parameter Fit

Temp °C	k_{23} 10^{-8}	k_{32} 10^{-7}	K_2	K_1
6	3.25	3.40	9.5	19.3
10	2.78	6.21	4.48	33.0
17	3.84	7.1	5.43	21.9
25	2.89	12.3	2.4	34.

$E_{32} = 11.0 \pm 1$ Kcal/mole

We will now discuss the other possibility, namely, that the observed relaxation is due to the first step, before we make a conclusion concerning the case we have just discussed. If the first step is the perturbed equilibrium, eq 2.C.39 must hold. τ_1^{-1} are plotted versus $[\overline{A}]$ (see Fig. 11) and straight lines are obtained at all temperatures. From the slopes and the intercepts the values of the forward, k_{12}, and backward, k_{21}, rate constants for the first step are evaluated (see Table VII). K_1 and K_2 are also calculated.

Table VII. Rate Constants of the First Step and Equilibrium Constants for the First and Second Steps Using Two-step Model

Temp °C	k_{12}^{d} x 10^{-9} C^{-1} sec^{-1}	k_{12} x 10^{-9} C^{-1} sec^{-1}	k_{21} x 10^{-8} sec^{-1}	K_1 C^{-1}	K_2
6	2.47	1.50 ± .23	1.25 ± .08	12.	16.
10	2.68	1.58 ± .24	1.55 ± .09	10.2	16.7
17	3.14	1.65 ± .25	1.90 ± .18	8.7	15.2
25	3.69	1.00 ± .55	2.52 ± .35	3.97	27.7

k_{12}^{d} is the theoretical diffusion rate constant, explained later.

The energies of activation for association and dissociation in the first step are evaluated from the temperature dependence of the rate constants using the Arrhenius equation

$$k = A \exp(-E_a/RT) \qquad (5.12)$$

Only the rate constants at 6, 10 and 17°C are used in these calculations. The values at 25°C were not used due to the high uncertainty at this

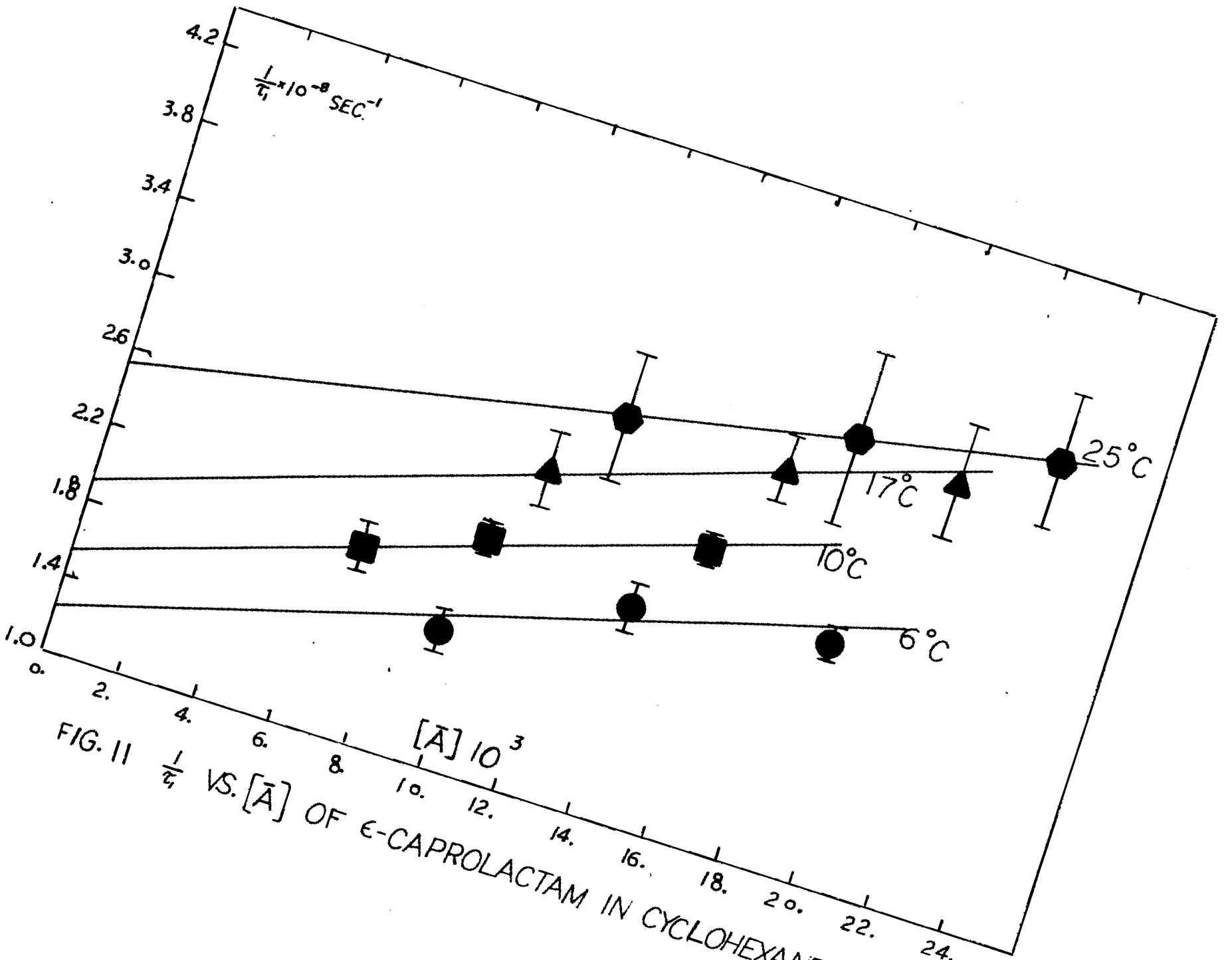

FIG. 11 $\frac{1}{\tau_1}$ VS. [Ā] OF ε-CAPROLACTAM IN CYCLOHEXANE

temperature. Table VIII contains the forward and backward energies of activation for the first step. The errors were calculated from the highest and lowest possible slopes. Errors in E_{12}, however, could be greater than the reported values due to the very small change of k_{12} with temperature.

Table VIII. Energies of Activation and Enthalpy Change for the First Step

$E_{12} = 1.31 \pm .50$ Kcal/mole--open dimer

$E_{21} = 6.20 \pm .30$ Kcal/mole--open dimer

$\Delta H^{o}_{12} = -4.9 \pm .8$ Kcal/mole--open dimer

We have seen that the experimental data fit both eqs 2.C.39 and 2.C.41. Thus the observed single relaxation could be due to the perturbation of the first or the second step. We feel, however, that it is more likely to be due to the first step for the following reasons. The forward rate constants of the first step k_{12} (Table III) and those of the second step k_{23} (Table VI) are almost constant within the expected errors ($\sim$ 15%) in the temperature range 6 to 17°C. Due to the fact that the first step association rate constant is diffusion controlled, as shown later, and that the second step, k_{23}, is a formation of one H-bond, it is more likely that k_{23} should increase more with increasing

temperature than k_{12}. Next we further evaluate the two-step model to show why the observed relaxation is preferably assigned due to the first step.

Evaluation of the Model.

A complete evaluation of this model would be possible only if a complete analysis of the two steps were obtained. This would have been possible if the two relaxations were observed. Due to the fact that the observed relaxation is more likely to be due to the perturbation of the first step, a complete analysis can only be done for that step. One way to check the model under the present conditions is to see whether the rates of forming the open dimer, k_{12}, are indeed diffusion controlled rates. In order to do this we calculate the theoretical rates for the dimerization using equation 5.13.[38]

$$k_{12}^{d} = 4RT/3000\eta \qquad (5.13)$$

where k_{12}^{d} is the diffusion rate constant (we used as k_{12} in our treatment), R is the gas constant (8.31432×10^{7} erg K^{-1}), T is the absolute temperature and η the viscosity of the medium.

In calculating k_{12}^{d} the viscosities used are those obtained from the literature[39] for pure cyclohexane (Fig. 12). The calculated values of k_{12}^{d} are shown along with k_{12} in Table VII. If we now compare k_{12} values obtained from our model to those calculated theoretically (Table VII) we can see the agreement. This agreement is even better than it appears since 5.13 is derived assuming that for each encounter a reaction takes place. Therefore, the theoretical values must be considered as the maximum possible rates. Normal steric effects could easily decrease them to the experimental values. It is also shown that the variation of k_{12}^{d} in the range 6 to 17°C is no more than 25% of the value at 6°C. This

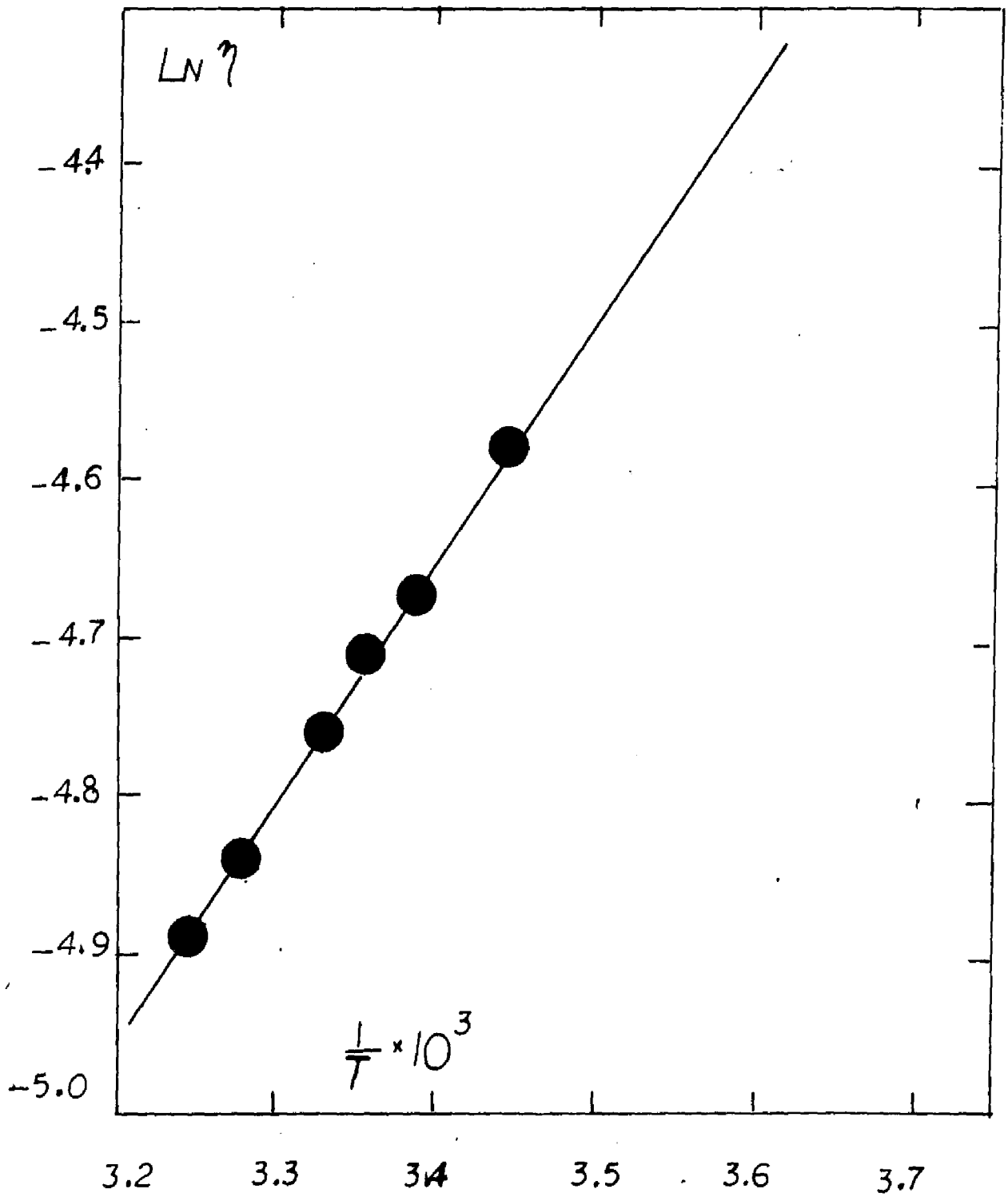

FIG.12 Ln η VS. 1/T OF CYCLOHEXANE

then explains the small change observed in our values of k_{12} with temperature considering the errors in these values.

Another way of checking our model is to calculate ΔH^{o} from the amplitudes (using 5.14 which is derived from A in eq 2.D.31) and compare its value to that obtained from the kinetic results.

$$\left(\Delta H^{o} - \frac{C_p \Delta V^{o}}{V\theta}\right) = \left\{ A f_c \sum \nu_i^2 / c_i \cdot \frac{C_p v R T^2}{\pi(\gamma - 1)V} \right\}^{1/2} \qquad (5.14)$$

where all the symbols in eq 5.14 are defined in Chapter II.

In eq 5.14 we can assume that the volume change of the dimerization is negligible. Using the physical constants (as reported in the literature[18,39] and listed in Table IX) of pure cyclohexane, we calculate ΔH^{o} at 17°C to be -8.6 Kcal/mole. This value is the average of three values

Table IX. Physical Constants of Pure Cyclohexane at 17°C

C_p	= 36.8 cal $mole^{-1}$ deg^{-1}	V	= 108 $m/mole^{-1}$
v	= 1.294 x 10^5 cm sec^{-1}	θ	= 1.208 deg^{-1}
T	= 290.15°K	$\gamma - 1$	= .387

calculated at three concentrations. The possible error introduced by assuming that the volume change of the association process is negligible may be calculated. If ΔV were as large as -3 ml $mole^{-1}$, for example, then $C_p \Delta V/\theta V$ = -.8 Kcal/mole, which will make ΔH^{o} = -7.8 Kcal/mole. There are, however, two more ways to introduce errors into ΔH^{o}. The first is errors in K_1 (used to calculate c_i's) which are estimated at about 30%. The second is the contribution of the second step to the amplitudes of the first step. Considering these various effects, the

ΔH^{o} values obtained from the kinetic treatment ($-4.9 \pm .8$) and that obtained from the amplitudes (-7.8 Kcal/mole) are in agreement qualitatively. Qualitative rather than quantitative agreement is not unexpected here since the existence of any errors in the K values will be amplified when used to calculate ΔH, since ΔH is the derivative of ln K.

CHAPTER VI

SUMMARY AND CONCLUSION

A. Summary

The ultrasonic absorption technique has been used to study the kinetics of ε-caprolactam association in cyclohexane solutions at 6, 10, 17 and 25°C. A single relaxation process is observed and attributed to the presence of a chemical equilibrium between monomers and dimers of ε-caprolactam.

Two models are shown to fit the experimental data within experimental error. The first consists of the formation of the cyclic dimer (2 H-bonds) in one step. The second is the formation of the same cyclic dimer in two steps. The first model was ruled out on the grounds that the association equilibrium constants calculated from the rate constants are inconsistent with the equilibrium constants obtained from the IR spectroscopy. The second model is used with the condition that the first step equilibrates faster than the second step. In principle two relaxation processes should be observed if a wide range of frequencies is studied and the two processes have reasonable amplitudes. Since only one relaxation process has been observed, assignment of this relaxation must be made.

We showed that the observed relaxation process is due to the perturbation of the first step.

Using the equilibrium constants obtained from the IR data as the overall one of the process, we calculate the rate constants of the

first step and the equilibrium constants of both steps (see Table XXV).

Table X. Summary of the Kinetics and Equilibrium Constants for the Two-Step Model

	First Step			Second Step	Overall
Temp °C	k_{12} 10^{-9} l $M^{-1}sec^{-1}$	k_{21} 10^{-8}	K_1 M^{-1} l	K_2	K_{IR}
6	1.5	1.25	12.0	16	204
10	1.58	1.55	10.2	16.7	181
17	1.65	1.90	8.7	15.2	141
25	1.00	2.52	9.2	11.4	114

The forward rate constants are in agreement with those calculated theoretically from the diffusion rate equation. This suggests, along with the small activation energy (E_{12} = 1.3 ± .5 Kcal/mole), that this forward step is a diffusion controlled process. This conclusion is in agreement with previous work done by several authors on H-bond polymerization in organic solvents.

B. Conclusion

1. It is concluded from this work that the cyclic dimer of ε-caprolactam in cyclohexane is formed in two steps.

2. The two steps equilibrate with different rates, the first step equilibrating faster than the second.

3. The observed relaxation process is due to the perturbation of the first step.

4. The formation of the open dimer is a diffusion-controlled step with energy of activation 1.3 ± .5 Kcal/mole--open dimer.

5. 6.2 ± .3 Kcal are needed to break the N—H - - - O H-bond in the open dimer of ε-caprolactam in cyclohexane.

6. The formation and rupture of H-bonds of N—H - - - O type is extremely fast, which also implies that the elementary steps in structural changes in nucleic acids, proteins and polypeptides are very fast.

7. The stability of the N—H - - - O H-bond is on the order of 4-5 Kcal/mole.

Conclusions 4 to 7 are consistent with the very small amount of data available in systems similar to the one under investigation.

APPENDIX A

RELATION BETWEEN THE RELAXATION STRENGTH AND THERMODYNAMIC PARAMETERS

If we have a chemical reaction specified by the stoichiometric formula

$$\sum \nu_i M_i = 0 \tag{A.1}$$

where ν_i is the stoichiometric coefficient of the ith species of M. The change in mole numbers of the ith constituent due to the reaction is

$$dN_i = \nu_i d\zeta \tag{A.2}$$

where N is the number of moles and ζ is the ordering parameter, or extent of reaction.

The dependent thermodynamic variables of such reaction are the entropy, S, volume, V, and the affinity are conjugate to the independent variables T, P and ζ, respectively. At equilibrium the following relation holds:

$$[\partial G/\partial \zeta]_{P,T} = 0 \tag{A.3}$$

where $G = G(P,T,\zeta)$ is the Gibbs free energy.

The affinity A is a measure of the departure of the system from equilibrium and is given by

$$A = -\sum_i \nu_i \mu_i \tag{A.4}$$

where μ_i represents chemical potentials.

Thus, the change in the Gibbs function (ΔG), due to the reaction

per unit change in ζ at constant pressure and temperature is given by

$$-\Delta G = [\partial G/\partial \zeta]_{P,T} = -A \qquad (A.5)$$

Let's define three, well-known, derivative properties in terms of both dependent and independent variables

Expansion coefficient $\theta = 1/V[\partial V/\partial T]_P$ (A.6)

Adiabatic compressibility $\beta_s = -1/V[\partial V/\partial P]_S$ (A.7)

Specific heat $C_P = T[\partial S/\partial T]_P$ (A.8)

Each of these three quantities can be written as summation of two quantities, for example

$$C_P = C_{P\infty} + \delta C_P \qquad (A.9)$$

where $C_{P\infty}$ is the instantaneous value of heat capacity at fixed ζ, which is given by

$$C_{P\infty} = T(\partial S/\partial T)_{P,\zeta} \qquad (A.10)$$

and δC_P is the difference between C_P and $C_{P\infty}$.

One can also write equations similar to A.9 and A.10 for θ, β_T and β_S.

The variation in the dependent variables (dS, dV, . . . dA) are given by

$$dS = (\partial S/\partial T)_{P,\zeta} dT + (\partial S/\partial P)_{T,\zeta} dP + (\partial S/\partial \zeta)_{P,T} d\zeta \qquad (A.11)$$

Using Maxwell's relation

$$(\partial S/\partial P)_{T,\zeta} = -(\partial V/\partial T)_{P,\zeta} \qquad (A.12)$$

and A.10, we get

$$dS = (C_{P\infty}/T)dt - V\theta^{\infty} dP + (\Delta H/T)d\zeta \qquad (A.13)$$

Also,

$$dV = (\partial V/\partial T)_{P,\zeta}dT + (\partial V/\partial P)_{T,\zeta}dP + (\partial V/\partial \zeta)_{P,T}d\zeta$$

$$= V\theta_{\infty}dT - V\beta_{T\infty}dP + \Delta V d\zeta \qquad (A.14)$$

and

$$dA = (\partial A/\partial T)_{P,\zeta}dT + (\partial A/\partial P)_{T,\zeta}dP + (\partial A/\partial \zeta)_{P,T}d\zeta \qquad (A.15)$$

From Maxwell's relations

$$\begin{aligned} [\partial A/\partial T]_{P,\zeta} &= [\partial S/\partial \zeta]_{P,T} = \Delta H/T \\ [\partial A/\partial P]_{T,\zeta} &= -(\partial V/\partial \zeta)_{P,T} = -\Delta V \end{aligned} \qquad (A.16)$$

Equation A.15 becomes

$$dA = (\Delta H/T)dT - \Delta V dP + \varphi d\zeta \qquad (A.17)$$

where φ is an ordering coefficient and is given by

$$\varphi = [\partial A/\partial \zeta]_{P,T} = -\sum_i \sum_j \nu_i \nu_j (\partial \mu_i/\partial N_j)_{P,T} \qquad (A.18)$$

When ζ is fixed, i.e., we are dealing with the instantaneous values, thus

$$(dS)_{\zeta} = (C_{P\infty}/T)dT - V\theta_{\infty}dP \qquad (A.19)$$

$$(dV)_{\zeta} = V\theta_{\infty}dT - V\beta_{T\infty}dP \qquad (A.20)$$

If changes are made slowly so that ζ is allowed to reach its equilibrium value at each instant, i.e., $A = 0$ or $dA = 0$, then

$$0 = (\Delta H/T)dT - \Delta V dP + \varphi d\zeta \quad .$$

On rearranging, we have

$$d\zeta = 1/\varphi[\Delta V dP - (\Delta H/T)dT] \qquad (A.21)$$

Substituting in A.13 and A.14 by A.21, we get

$$(dS)_A = \left\{1/T[C_{P\infty} - \Delta H^2/T\varphi]\right\}dT - \left\{V[\theta_\infty - \Delta H\Delta V/TV\varphi]\right\}dP \quad (A.22)$$

$$(dV)_A = \left\{V[\theta_\infty - \Delta H\Delta V/T\varphi V]\right\}dT - \left\{V[\beta_{T\infty} - \Delta V^2/\varphi V]\right\}dP \quad (A.23)$$

From A.10

$$\delta C_P = C_P - C_{P\infty} = T(\partial S/\partial T)_{P,A} - T(\partial S/\partial T)_{P,\zeta} \quad (A.24)$$

Also,

$$\delta\theta = \theta - \theta_\infty = 1/V(\partial V/\partial T)_{P,A} - 1/V(\partial V/\partial T)_{P,\zeta} \quad (A.25)$$

and

$$\delta\beta_s = \beta_s - \beta_{s\infty} = 1/V(\partial V/\partial P)_{s,A} - 1/V(\partial V/\partial P)_{s,\zeta} \quad (A.26)$$

Equations A.22 and A.23 can be written

$$(dS)_A = C_P/T - V\theta dP \quad (A.27)$$

and

$$(dV)_A = V\theta dT - V\beta_T dP \quad (A.28)$$

Now, comparison of A.27 with A.22 and A.28 with A.23 gives the excess properties

$$\delta C_P = -\Delta H^2/T\varphi$$

$$\delta\theta = -\Delta H^2/T\varphi V$$

$$\delta\beta_T = -\Delta V^2/\varphi V \quad (A.29)$$

From these three relations we find

$$\delta\beta_T\delta C_P = TV(\delta\theta)^2 \quad (A.30)$$

but the adiabatic compressibility is related to the isothermal one by

$$\beta_s = \beta_T - T\theta^2V/C_P \quad (A.31)$$

Thus

$$\delta\beta_s = \delta\beta_T - TV\delta(\theta^2/C_P) \quad (A.32)$$

Using A.30 and

$$(\gamma - 1) = TV\theta^2/C_P\beta_s \quad (A.33)$$

we get

$$\delta\beta_s/\beta_s = (\gamma - 1)[\delta\theta/\theta - \delta C_P/C_P]^2/\delta C_P/C_P[1 - \delta C_P/C_P] \quad (A.34)$$

$$= [C_P/C_{P\infty}]\ (\delta\theta_T/\theta_s)^{1/2} - [(\gamma - 1)\delta C_P/C_P]^{1/2\ 2} \qquad (A.35)$$

Let $\delta\theta_s = \theta_r$ and $\theta_s = \theta_o$ arranging and using the above equations we get

$$\frac{\theta_r}{\theta_o} = \frac{(\gamma - 1)\delta C_P}{C_{P\infty}} \left(1 - \frac{\Delta V}{\Delta H}\ \frac{C_P}{V\theta}\right)^2 \qquad (2.D.26)$$

where θ_r/θ_o is the relaxation strength.

APPENDIX B

CALCULATION OF ABSORPTION COEFFICIENT (α)

1. Least Squares Analysis of Straight Line

The least squares method, in general, is a mathematical method of finding the "best" values of the constants in a given type of equation to fit the experimental data as well as possible. The criterion for the "best" fit is that the sum of the squares of the deviations of the experimental points from the chosen line should be as small as possible; this can be shown to correspond to the condition that the arithmetic mean should be the "best" representation of a series of readings of the same quantity. It would hold if the deviations from the line followed the normal errors distribution. The method is applicable to many forms of equations. In this appendix we are considering a two-parameter fit to a straight line. In Appendix C a three-parameter fit is considered.

Suppose the data consist of a set of n points, the coordinates of which (x_1y_1, x_2y_2, . . . x_n,y_n) are tabulated. In correspondence to our measurements x_i is the distance in cm and y_i is the attenuation at the corresponding distance. By hypothesis these results are scattered at random from the "true" line, the equation of which is taken as

$$y = a + bx \quad .$$

Suppose that the values of the independent variable x can be regarded as subject to negligible error, all the deviations being in the y values. The y deviations can then be written down. Thus, for a typical point,

i, y_i should have been at $(a + bx_i)$, and the deviation is therefore $y_i - (a + bx_i)$. The sum of the squares of the deviations is $\Sigma(y_i - a - bx_i)^2$ summed over all n points and this quantity must be minimized by suitable choice of a and b. The condition for a minimum is obtained by differentiating the expression with respect to a and b, putting the derivatives equal to zero and solving the resulting pair of simultaneous equations. The final working formulae for obtaining the "best" constants are[40]

$$a = \bar{y} - b\bar{x} \quad \text{and} \quad b = \frac{(x_i - \bar{x})(y_i - \bar{y})}{(x_i - \bar{x})^2}$$

where $\bar{y}$ is the mean value of y's $= \Sigma\, y_i/n$

$\bar{x}$ is the mean value of x's $= \Sigma\, x_i/n$.

It should be noted that in our particular case we are only interested in the slope, b, the absorption coefficient in decibels per cm.

The standard deviation in α.

It is given by

$$S = \left[\sum_{i=1}^{i=m} \frac{(\alpha_i - \bar{\alpha})^2}{m - 1} \right]^{1/2}$$

where S = standard deviation

m = the number of results

$\bar{\alpha}$ = the arithmetic average of the m results

and α = a single result.

2. Computer Program for Calculating α and S

```
      INTEGER M,L,N,I,K
      REAL LI,NI
      DIMENSION SI(5),XI(15),YI(15)
      WRITE (6,1005)
1005  FORMAT(1H1,3X,9HFREQUENCY,7X,6HA/F**2,8X,8HSLOPE AV,8X,8HALPHA AV
     1 ,7X,7HSTD DEV)
      READ(5,1006)M
      DO 90 K=1,M
      READ (5,1001)L
      DO 100 J=1,L
      READ (5,1001)N
      XT=0.
      YT=0.
      DO 110 I=1,N
      READ (5,1002)XI(I),YI(I)
      XT=XT+XI(I)
      YT=YT+YI(I)
110   CONTINUE
      NI=FLOAT(N)
      XB=XT/NI
      YB=YT/NI
      ST=0.
      SS=0.
      DO 120 I=1,N
      ST=ST+(XI(I)-XB)*(YI(I)-YB)
      SS=SS+(ABS(XI(I)-XB))**2.
120   CONTINUE
      SI(J)=ST/SS
100   CONTINUE
      LI=FLOAT(L)
      SK=0.
      DO 130 K1=1,L
      SK=SK+SI(K1)
130   CONTINUE
      SAV=SK/LI
      ALPB=SAV/8.686
      AL=0.
      ALP=0.
      DO 140 I=1,L
      AL=AL+ABS(SI(I)/8.686)**2.
      ALP=ALP+ABS(SI(I)/8.686)
140   CONTINUE
      SD=SQRT((AL-((ALP)**2./LI))/(LI-1.))
      READ(5,1003)F
      AFSQ=ALPB/(F**2.)
      WRITE(6,1004)F,AFSQ,SAV,ALPB,SD
90    CONTINUE
1006  FORMAT(I2)
1001  FORMAT(I1)
1002  FORMAT(2E15.6)
1003  FORMAT(E15.6)
1004  FORMAT(1H ,5E15.8)
      STOP
      END
```

Symbols used in the computer program evaluating α and S.

M = number of frequencies in the run for each concentration at each temperature.

L = number of slopes for each set at each frequency.

N = number of points (readings) for each set of readings at each frequency.

LI = L

NI = N

XT = the sum of the cm (distances) for each set.

YT = the sum of the db (decibels) for each set.

XB = average cm (distance).

YB = average db (decibels).

XI(I) = the distance (cm) at each reading for one set.

YI(I) = the corresponding (db) readings.

ST = the sum of (XI(I)-XB)(YI(I)-YB).

SS = the sum of $(XI(I)-XB)^2$.

SI(J) = ST/SS = slope from the least squares method for each set.

SK = the sum of the slopes (ST) for each frequency.

SAV = average slope for each frequency determined by SK/total number of sets of readings at one frequency.

ALPB = absorption coefficient (average) = $\bar{\alpha}$ = SAV/8.686.

AT = sum of $(\alpha - \bar{\alpha})^2$ = $(SI/8.686 - ALPB)^2$.

SD = standard deviation of α = $\{ AT/\text{number of } \alpha\text{'s} - 1.0 \}^{1/2}$.

F = frequency; AFSQ = α/f^2 .

APPENDIX C

CALCULATION OF A, B and f_c

1. Least Squares Method for Calculating A, B and f_c

Consider the single relaxation equation

$$y = \alpha/f^2 = \frac{A}{1 + (f/f_c)^2} + B \qquad (2.D.31)$$

Here, y is linear in A and B but nonlinear in f_c. In order to have y linear in A, B and f_c, we use the same mathematical technique as R. Kay[41] in his treatment of the Debye-Onsager equation for conductance. Equation 2.D.31 can be rewritten as

$$y = \text{func.}\ (A, B, f_c) \qquad (App.C.1)$$

$$\text{Then,} \quad \Delta y_i = (\partial y_i/\partial A)\Delta A + (\partial y_i/\partial f_c)\Delta f_c + (\partial y_i/\partial B)\Delta B \qquad (App.C.2)$$

$$\text{where} \quad \Delta y_i = y_{\text{observed}} - y(i)_{\text{calculated}} \,. \qquad (App.C.3)$$

Now we can see that equation App.C.2 is linear in ΔA, Δf_c and ΔB.

If there are n measurements of y_{observed}, then n equations of the form App.C.2 can be obtained, and the best linear unbiased estimates ΔA, Δf_c, ΔB can be given by the solution of the three simultaneous equations called the normal equations,

$$\Sigma\left(\Delta y \frac{\partial y}{\partial A}\right) = \Sigma\left(\frac{\partial y}{\partial A}\right)^2 \Delta A + \Sigma\left(\frac{\partial y}{\partial A}\frac{\partial y}{\partial f_c}\right)\Delta f_c + \Sigma\ \frac{\partial y}{\partial A}\frac{\partial y}{\partial B}\ \Delta B$$

$$\Sigma\left(\Delta y \frac{\partial y}{\partial f_c}\right) = \Sigma\left(\frac{\partial y}{\partial A}\frac{\partial y}{\partial f_c}\right)\Delta A + \Sigma\left(\frac{\partial y}{\partial f_c}\right)^2 \Delta f_c + \Sigma\ \frac{\partial y}{\partial B}\frac{\partial y}{\partial f_c} \qquad (App.C.4)$$

and

$$\Sigma\ \Delta y \frac{\partial y}{\partial B} = \Sigma \left(\frac{\partial y}{\partial A}\frac{\partial y}{\partial B}\right)\Delta A + \Sigma\left(\frac{\partial y}{\partial f_c}\frac{\partial y}{\partial B}\right)\Delta f_c + \Sigma \left(\frac{\partial y}{\partial B}\right)^2 \Delta B$$

where the summation is overall of the n values of the variables involved.

Using 2.D.31 the derivatives in App.C.4. of y with respect to A, f_c and B can be given as

$$\partial y/\partial A = \partial/\partial A\left[\frac{A}{1 + (f/f_c)^2} + B\right] = \frac{1}{1 + (f/f_c)^2}$$

$$\partial y/\partial f_c = \partial/\partial f_c\left[\frac{A}{1 + (f/f_c)^2} + B\right] = \frac{\partial A f_c f^2}{(f_c^2 + f^2)^2}$$

and $$\partial y/\partial B = \partial/\partial B\left[\frac{A}{1 + (f/f_c)^2} + B\right] = 1 \qquad \text{(App.C.5)}$$

The normal equations can be rewritten in the following form.

$$\begin{aligned} s_7 &= s_1\Delta A + s_2\Delta f_c + s_3\Delta B \\ s_8 &= s_2\Delta A + s_4\Delta f_c + s_5\Delta B \\ s_9 &= s_3\Delta A + s_5\Delta f_c + s_6\Delta B \end{aligned} \qquad \text{(App.C.6)}$$

where the values of s's are defined from App.C.4. The set of equations App.C.6 can be written in the matrix form

$$X\beta = Y$$

where $Y = \begin{bmatrix} s_7 \\ s_8 \\ s_9 \end{bmatrix}$, $X = \begin{bmatrix} s_1 & s_2 & s_3 \\ s_2 & s_4 & s_5 \\ s_3 & s_5 & s_6 \end{bmatrix}$ and $\beta = \begin{bmatrix} \Delta A \\ \Delta f_c \\ \Delta B \end{bmatrix}$

The solution of the above set of equations can be solved by a number of methods giving values for ΔA, ΔB and Δf_c, which can be expressed (in the matrix form) as

$$\beta = X^{-1}Y$$

where X^{-1} is the inverse of the matrix, X, of the normal equations and is given by

$$X^{-1} = \begin{bmatrix} c_{11} & c_{12} & c_{13} \\ c_{21} & c_{22} & c_{23} \\ c_{31} & c_{32} & c_{33} \end{bmatrix}$$

where the c_{ij}'s are the elements of the inverse matrix X^{-1}.

The procedure, then, is to estimate values of A, B and f_c from a plot of α/f^2 vs log f. These estimates are used to calculate the theoretical curve and the partials $\partial y/\partial A$, $\partial y/\partial B$ and $\partial y/\partial f_c$. The sums in the normal equations are calculated, and the resulting expressions solved for ΔA, ΔB and Δf_c. These quantities are used to correct the initial estimates of the three constants.

The variance, S^2, of the fit is calculated from

$$S^2 = \Sigma \Delta y^2/(n - 3)$$

where n = number of data points and the standard deviation, S, of the fit is given by

$$S = \sqrt{\Delta y^2/(n - 3)}$$

The process was iterated until the standard deviation was constant to two decimal places or the difference between two successive values of standard deviations divided by the last one is constant to four decimal places or the number of iterations exceeds forty times.

Standard deviation of A, B and f_c.

The standard deviation of β_i (A, B or f_c) is given by

$$\beta_i = S\sqrt{c_{ii}}$$

where c_{ii} is the ith diagonal term of the inverse of the matrix of normal equations.

2. Computer Program for Calculating A, B and f_c

```
      INTEGER P
      DIMENSION AFC(25),AFC(25),F(25),Y(25)
      READ(5,40) N
40    FORMAT(I2)
      DO 10 INT=1,N
      READ(5,40)P
      READ(5,39)A,FC,B
39    FORMAT(F15.5,F15.5,F15.5)
      DO 50 J=1,P
38    FORMAT(2F15.5)
      READ(5,38)AFC(J),F(J)
      AFC(J)=A/(1.+(F(J)/FC)**2)+B
50    Y(J)=AFC(J)-AFC(J)
      AA=0.0
      CCONST =1.0
400   Y5=0.
      S1=0.
      S2=0.
      S3=0.
      S3=0.
      S4=0.
      S5=0.
      S5=0.
      S6=0.
      S7=0.
      S8=0.
      S9=0.
      DO 100 J=1,P
      Y1=1.0/(1.0+(F(J)/FC)**2)
      Y2=(2.0*A*FC*F(J)*F(J))/((FC*FC+F(J)*F(J))**2)
      Y3=1.0
      S1=S1+Y1*Y1
      S3=S3+Y1*Y3
      S2=S2+Y1*Y2
      S4=S4+Y2*Y2
      S5=S5+Y2*Y3
      S6=S6+Y3*Y3
      S7=S7+Y1*Y(J)
      S8=S8+Y2*Y(J)
      S9=S9+Y3*Y(J)
100   Y5=Y5+Y(J)*Y(J)
      DET  =(S1*(S4*S6-S5*S5)+S2*(S5*S3-S4*S2)+S3*(S2*S5-S4*S3))
      DETA =(S7*(S4*S6-S5*S5)+S8*(S5*S3-S6*S2)+S9*(S2*S5-S4*S3))
      DETFC=(S1*(S8*S6-S9*S5)+S2*(S3*S9-S6*S7)+S3*(S5*S7-S8*S3))
      DETB =(S1*(S4*S9-S5*S8)+S2*(S5*S7-S9*S2)+S3*(S2*S8-S4*S7))
      IF(DET.EQ.0.0) GO TO 14
      DA=DETA/DET
      DFC=DETFC/DET
      DB=DETB/DET
      A=A+DA
      FC=FC+DFC
      B=B+DB
      Y5=0.0
      DO 200 J=1,P
      AFC(J)=A/(1.0+(F(J)/FC)**2)+B
```

```
      Y(J)=AFC(J)-AFO(J)
200   YS=YS+Y(J)*Y(J)
      POINTS=FLOAT(P)
      STDDEV=SQRT(ABS(YS/(POINTS-3.0)))
      STDA=STDDEV*SQRT(ABS((S4*S6-S5*S5)/DET))
      STDFC=STDDEV*SQRT(ABS((S1*S6-S3*S3)/DET))
      STDB=STDDEV*SQRT(ABS((S1*S4-S2*S2)/DET))
      IF(COUNT.GT.40.0) GO TO 11
      AF=STDDEV
      IF(ABS((AF-AA)/AF).LE.0.0001) GO TO 11
      IF(STDDEV.LT..01) GO TO 11
      AA=AF
      COUNT=COUNT+1.0
      IF(A.GT.100000.0) GO TO 14
      IF(A.LT.0.0) GO TO 14
      GO TO 400
11    CONTINUE
      WRITE(6,41)
41    FORMAT(1H1,11X,9HFREQUENCY,6X,19HOBSERVED ALPHA/F**2,6X,21HCALCULA
     TED ALPHA/F**2)
      DO 300 J=1,P
      WRITE(6,42)F(J),AFO(J),AFC(J)
42    FORMAT(1H ,F20.5,F20.5,6X,F20.5)
300   CONTINUE
      WRITE(6,43)A,STDA
43    FORMAT(1H3,3H A=,F10.5,3X,3H+/-,F10.5)
44    FORMAT(1H ,3HFC=,F10.5,3X,3H+/-,F10.5)
45    FORMAT(1H ,3H B=,F10.5,3X,3H+/-,F10.5)
      WRITE(6,44)FC,STDFC
      WRITE(6,45)B,STDB
      WRITE(6,46)STDDEV
46    FORMAT(1H ,30HSTANDARD DEVIATION OF THE FIT=,F10.5)
      GO TO 10
14    WRITE(6,977)A,FC,B,DET
977   FORMAT(1H1,F15.8,F15.8,F15.8,F15.8)
10    CONTINUE
500   STOP
      END
```

Symbols used in the computer program for evaluating A, B and f_c.

AFO = observed values of α/f^2.

AFC = calculated values of α/f^2.

F = frequency.

Y = the difference between the observed and the calculated α/f^2.

N = number of runs (i.e., concentrations).

P = number of frequencies in each run.

A = amplitude.

FC = characteristic frequency.

B = background.

S1 = $\Sigma\ [\partial(\alpha/f^2)/\partial A]^2$

S2 = $\Sigma\ [\partial(\alpha/f^2)/\partial A][\partial(\alpha/f^2)/\partial f_c]$

S3 = $\Sigma\ [\partial(\alpha/f^2)/\partial A][\partial(\alpha/f^2)/\partial B]$

S4 = $\Sigma\ [\partial(\alpha/f^2)/\partial f_c]^2$

S5 = $\Sigma\ [\partial(\alpha/f^2)/\partial f_c][\partial(\alpha/f^2)/\partial B]$

S6 = $\Sigma\ [\partial(\alpha/f^2)/\partial B]^2$

S7 = $\Sigma\ [\partial(\alpha/f^2)/\partial A][Afo(J) - Afc(J)]$

S8 = $\Sigma\ [\partial(\alpha/f^2)/\partial f_c][Afo(J) - Afc(J)]$

S9 = $\Sigma\ [\partial(\alpha/f^2)/\partial B][Afo(J) - Afc(J)]$

Y1 = $\partial(\alpha/f^2)/\partial A$

Y2 = $\partial(\alpha/f^2)/\partial f_c$

Y3 = $\partial(\alpha/f^2)/\partial B$

Y5 = $\Sigma[Afo(J) - Afc(J)]^2$

J(J) = Afo(J) - Afo(J)

DET = $[S1(S4S6 - S5^2) + S2(S5S3 - S6S2) + S3(S2S5 - S4S3)]$

DETA = $[S7(S4S6 - S5^2) + S8(S5S3 - S6S2) + S9(S2S5 - S4S3)]$

DETFC = $[S2(S8S6 - S9S5) + S2(S3S9 - S6S7) + S3(S5S7 - S8S3)]$

$$DETB = [S_1(S4S9 - S5S8) + S2(S5S7 - S9S2) + S3(S2S8 - S4S7)]$$

$$DA = DETA/DET$$

$$DFC = DETFC/DET$$

$$DB = DETB/DET$$

$$A = \Sigma\ DA$$

$$FC = \Sigma\ DFC$$

$$B = \Sigma\ DB$$

$$AFC(J) = A/[1 + (F(J)/Fc)^2] + B$$

$$Y(J) = Afo(J) - Afc(J)$$

APPENDIX D

TABULATED EXPERIMENTAL AND CALCULATED RESULTS

Table XI. Measured Absorption of Pure Cyclohexane at 10°C

f MHz	α neper cm^{-1}	Standard deviation in α	$(\alpha/f^2)_{observed}$ 10^{17} sec^2 cm^{-1}
25.209	1.1439	.00281	180.0
45.3440	3.6830	.0251	179.1
65.6740	7.7220	.0227	179.0
85.8744	13.0391	.1042	176.8
95.9532	16.2412	.1907	176.5
106.0600	19.7977	.0945	176.1

The standard deviation = 1.64.

Measured Absorption of Pure Cyclohexane at 6, 10, 17 and 25°C

Temp °C	$(\alpha/f^2)_{observed}$ 10^{17} sec^2 cm^{-1}
6	176
10	178
17	188
25	198

Table XII. Measured Absorption of Pure Solvents* and ε-Caprolactam Solutions* in Various Solvents at 25°C

Solvent	$(\alpha/f^2)_{solvent}$ 10^{17} sec^2 cm^{-1}	$(\alpha/f^2)_{solution}$ 10^{17} sec^2 cm^{-1}	Concentration M
Water	21	22	.098
Toluene	85	100	.086
Dioxane	110	117	.097
Carbon tetrachloride	518	526	.193

* Data reported here are an average value of α/f^2 at various frequencies.

Table XIII. Measured and Calculated Absorption of .046 M ε-Caprolactam-Cyclohexane at 6°C

f MHz	α neper cm^{-1}	Standard deviation in α	$(\alpha/f^2)_{observed}$ 10^{17} sec^2 cm^{-1}	$(\alpha/f^2)_{calc.}$ 10^{17} sec^2 cm^{-1}
15.0556	.55987	.00401	247.0	246.3
25.2700	1.4176	.00654	222.0	223.9
35.3700	2.6022	.02795	208.0	207.9
45.6200	4.1291	.01802	198.4	197.4
55.6800	5.9835	.04405	193.0	190.8
65.7670	8.0061	.03914	185.1	186.3
75.8800	10.5425	.05119	183.1	183.3
85.9350	13.4404	.03013	182.0	181.1
96.0050	16.4062	.0550	178.0	179.5

Standard deviation of the fit = 1.56.

Table XIV. Measured and Calculated Absorption of .094 M ε-Caprolactam-Cyclohexane at 6°C

f MHz	α neper cm^{-1}	Standard deviation in α	$(\alpha/f^2)_{observed}$ 10^{17} sec^2 cm^{-1}	$(\alpha/f^2)_{calc.}$ 10^{17} sec^2 cm^{-1}
15.0560	.54857	.00484	242.0	241.1
25.2700	1.4317	.01047	224.2	225.6
35.3720	2.6450	.01660	211.4	212.5
45.6200	4.2310	.14070	203.3	202.8
55.6850	6.1396	.02615	198.0	196.1
65.7680	8.3048	.04813	192.0	191.4
75.8900	10.8851	.1091	189.0	188.0
85.9360	13.6401	.1861	184.7	185.5
95.9960	16.7809	.0319	182.1	183.7

Standard deviation of the fit = 1.44.

Table XV. Measured and Calculated Absorption of .15 M ε-Caprolactam-Cyclohexane at 6°C

f MHz	α neper cm^{-1}	Standard deviation in α	$(\alpha/f^2)_{observed}$ 10^{17} sec^2 cm^{-1}	$(\alpha/f^2)_{calc.}$ 10^{17} sec^2 cm^{-1}
15.0500	.54111	.00380	238.9	239.0
25.2000	1.4358	.00841	226.1	225.8
35.3700	2.6772	.01542	214.0	214.0
45.6000	4.2523	.02112	204.5	204.9
55.6000	6.1642	.03142	199.4	198.5
65.7600	8.3460	.04081	193.0	193.8
75.8800	10.9455	.08261	190.1	190.4
85.9400	13.8482	.16542	187.5	187.9
96.0000	17.2155	.14303	186.8	186.0

Standard deviation of the fit = .654.

Table XVI. Measured and Calculated Absorption of .026 M ε-Caprolactam-Cyclohexane at 10°C

f MHz	α neper cm^{-1}	Standard deviation in α	$(\alpha/f^2)_{observed}$ 10^{17} sec^2 cm^{-1}	$(\alpha/f^2)_{calc.}$ 10^{17} sec^2 cm^{-1}
15.01	.56145	.0044	249.2	247.9
25.270	1.4432	.0557	226.0	229.5
35.31	2.6993	.0210	216.5	215.3
45.46	4.2696	.0167	206.6	205.2
55.47	6.1292	.0345	199.2	198.5
65.68	8.3258	.0172	193.0	193.8
85.86	13.8887	.0470	188.4	188.3
96.014	17.1468	.2292	186.0	186.5
106.100	20.7133	.1143	184.0	185.2

Standard deviation of the fit = 2.2.

Table XVII. Measured and Calculated Absorption of .05 M ε-Caprolactam-Cyclohexane at 10°C

f MHz	α neper cm^{-1}	Standard deviation in α	$(\alpha/f^2)_{observed}$ 10^{17} sec^2 cm^{-1}	$(\alpha/f^2)_{calc.}$ 10^{17} sec^2 cm^{-1}
15.1020	.53847	.00623	236.1	234.0
25.2600	1.4114	.01140	221.2	221.4
35.3000	2.6168	.02401	210.0	210.2
45.600	4.2211	.03178	203.0	201.9
55.508	6.0298	.0276	195.7	195.5
65.680	8.2395	.0964	191.0	191.1
86.010	13.7154	.07325	185.4	185.5
96.000	16.9205	.04014	183.6	183.8
116.1023	24.4513	.3423	181.5	181.4

Standard deviation of the fit = .4.

Table XVIII. Measured and Calculated Absorption of .103 M

ε-Caprolactam-Cyclohexane at 10°C

f MHz	α neper cm^{-1}	Standard deviation in α	$(\alpha/f^2)_{observed}$ 10^{17} sec^2 cm^{-1}	$(\alpha/f^2)_{calc.}$ 10^{17} sec^2 cm^{-1}
15.050	.50872	.0025	224.6	224.7
25.27	1.3736	.0054	215.1	215.0
35.30	2.5669	.00356	206.0	205.9
45.46	4.0960	.01610	198.2	198.5
55.500	5.9664	.0542	193.7	192.9
65.670	8.1162	.0392	188.2	188.7
85.850	13.4875	.0310	183.0	183.3
116.102	24.1825	.1041	179.4	179.1

Standard deviation of the fit = .5.

Table XIX. Measured and Calculated Absorption of .05 M

ε-Caprolactam-Cyclohexane at 17°C

f MHz	α neper cm^{-1}	Standard deviation in α	$(\alpha/f^2)_{observed}$ 10^{17} sec^2 cm^{-1}	$(\alpha/f^2)_{calc.}$ 10^{17} sec^2 cm^{-1}
25.1600	1.3464	.0803	212.7	212.9
35.3000	2.5869	.0138	207.6	207.4
45.4700	4.1888	.0221	202.6	202.6
55.6000	6.1827	.0199	200.0	198.7
65.6180	8.3660	.0443	194.3	195.8
75.7400	11.0715	.0338	193.0	193.5
85.8460	14.1127	.0869	191.5	191.7
95.9380	17.5982	.0588	191.2	190.3

Standard deviation of the fit = .99.

Table XX. Measured and Calculated Absorption of .096 M ε-Caprolactam-Cyclohexane at 17°C

f MHz	α neper cm^{-1}	Standard deviation in α	$(\alpha/f^2)_{observed}$ 10^{17} sec^2 cm^{-1}	$(\alpha/f^2)_{calc.}$ 10^{17} sec^2 cm^{-1}
25.270	1.4374	.00454	225.1	225.4
35.371	2.7174	.01653	217.2	216.9
45.62	4.3663	.02698	209.8	209.3
55.68	6.3121	.0474	203.6	203.1
65.76	8.4974	.03277	196.5	198.3
75.98	11.1822	.0708	193.7	194.4
85.90	14.2116	.0474	192.6	191.5
96.00	17.5104	.0884	190.0	189.1
106.03	21.0457	.10968	187.2	187.3
116.08	25.0762	.16193	186.1	185.8
126.22	29.2980	.23199	183.9	184.6

Standard deviation of the fit = .92.

Table XXI. Measured and Calculated Absorption of .15 M ε-Caprolactam-Cyclohexane at 17°C

f MHz	α neper cm^{-1}	Standard deviation in α	$(\alpha/f^2)_{observed}$ 10^{17} sec^2 cm^{-1}	$(\alpha/f^2)_{calc.}$ 10^{17} sec^2 cm^{-1}
15.0556	.53494	.000273	236.0	233.1
25.2680	1.4366	.009476	225.	227.5
35.3700	2.7398	.03086	219.0	221.2
45.6200	4.4766	.02286	215.1	215.1
55.6800	6.4826	.05436	209.1	209.9
65.7650	8.9355	.07684	206.6	205.6
75.8800	11.7459	.66501	204.0	202.1
85.9350	14.8139	.26059	200.6	199.3
96.005	18.3786	.18373	199.4	197.0
116.0800	26.0463	.15908	193.3	193.7
126.2420	30.1369	.29326	189.1	192.5

Standard deviation of the fit = 2.34.

Table XXII. Measured and Calculated Absorption of .048 M ε-Caprolactam-Cyclohexane at 25°C

f MHz	α neper cm^{-1}	Standard deviation in α	$(\alpha/f^2)_{observed}$ 10^{17} sec^2 cm^{-1}	$(\alpha/f^2)_{calc.}$ 10^{17} sec^2 cm^{-1}
25.2700	1.4866	.00756	232.8	231.4
35.3700	2.7773	.02428	222.0	224.3
45.6300	4.5223	.04103	217.2	217.8
55.6860	6.6236	.03139	213.6	212.6
65.7680	9.0401	.12493	209.0	208.4
75.8900	11.8526	.08555	205.8	205.1
85.9360	14.9694	.09316	202.7	202.5
95.9960	18.4305	.14063	200.0	200.4
106.0320	22.4631	.13772	199.8	198.8
116.0800	26.4102	.21313	196.0	197.5

Standard deviation of the fit = 1.38.

Table XXIII. Measured and Calculated Absorption of .096 M ε-Caprolactam-Cyclohexane at 25°C

f MHz	α neper cm^{-1}	Standard deviation in α	$(\alpha/f^2)_{observed}$ 10^{17} sec^2 cm^{-1}	$(\alpha/f^2)_{calc.}$ 10^{17} sec^2 cm^{-1}
25.270	1.4738	.00309	230.8	229.9
35.3700	2.7823	.01109	222.4	224.0
45.6300	4.5640	.05098	219.2	218.5
55.6800	6.5726	.03754	212.0	213.9
65.7600	9.1504	.1367	211.6	210.1
75.8900	11.9793	.15907	208.0	207.1
85.9300	15.1076	.05211	204.6	204.7
96.0000	18.7361	.1603	203.3	202.8
106.0300	22.7433	.1498	202.3	201.3
116.0800	26.7066	.2349	198.2	200.1

Standard deviation of the fit = 1.47.

Table XXIV. Measured and Calculated Absorption of .148 M ε-Caprolactam-Cyclohexane at 25°C

f MHz	α neper cm^{-1}	Standard deviation in α	$(\alpha/f^2)_{observed}$ 10^{17} sec^2 cm^{-1}	$(\alpha/f^2)_{calc.}$ 10^{17} sec^2 cm^{-1}
15.0560	.54404	.00808	240.0	238.0
25.1680	1.4645	.00554	231.2	232.2
35.472	2.8110	.02223	223.4	225.5
55.608	6.7318	.02808	217.7	219.0
65.6100	9.1733	.09797	213.1	213.4
75.7470	12.0719	.06426	210.4	208.8
85.8450	15.1956	.03935	206.2	204.9
96.0000	18.7085	.16030	203.0	201.9
106.1400	22.5990	.25792	200.6	199.4
116.1400	26.5723	.32019	197.9	197.4
126.1000	30.2600	.22699	197.0	195.8
			190.3	194.5

The standard deviation of the fit = 2.0.

APPENDIX E

COMPUTER PROGRAM FOR THE TWO-PARAMETER FIT

```
      REAL K,K23,K32,K1,K2
       DIMENSION A(3),Y(3),RIS(3),YC(3)
      DO 200  J=1,4
      READ(5,1)K,K23,K32
      READ(5,2)(A(I),I=1,3),(Y(I),I=1,3)
      WRITE(6,3)
      OLDVAR=0.
      KOUNT=1
110   VAR=0.
      DO 101 I=1,3
      YC(I)=((K23+K32)-K23*((K23+K32)/((4.*K32*K*A(I))+K23+K32)))
      RIS(I)=Y(I)-YC(I)
101   VAR=VAR+RIS(I)*RIS(I)
      K2=K23/K32
      K1=K/(K2+1.)
      WRITE(6,4)K,K1,K2,K23,K32,VAR
      IF(KOUNT.GT.40)GO TO 100
      IF((VAR-OLDVAR)/VAR.LT.0.001)GO TO 100
      S1=0.
      S2=0.
      S3=0.
      S4=0.
      S5=0.
      VAR=0.
      DO 103 I=1,3
      D1=1.-K23* ((4.*K32*K*A(I))/(4.*K32*K*A(I)+K23+K32)**2 )-((
     1 K23+K32)/(4.*K32*K*A(I)+K23+K32))
      D2=1.+K23*((4.*K*A(I)*K23)/((4.*K32*K*A(I)+K23+K32)**2 ))
      S1=S1+D1*D1
      S2=S2+D1*D2
      S3=S3+D2*D2
      S4=S4+D1*RIS(I)
      S5=S5+D2*RIS(I)
103   VAR=VAR+RIS(I)*RIS(I)
      DET=S1*S3-S2*S2
      DETA=S4*S3-S5*S2
      DETB=S1*S5-S2*S4
      IF(ABS(DET).LT.1.E-20)GO TO 100
      K23=K23+DETA/DET
      K32=K32+DETB/DET
      KOUNT=KOUNT+1
      GO TO 110
100   DO 104 I=1,3
```

```
104     WRITE(6,5)Y(I),YC(I)
1       FORMAT(F15.5,1P2E15.5)
2       FORMAT(3F15.5/1P3E15.5)
3       FORMAT(1H1)
 4      FORMAT(1HO,1P6E15.5)
5       FORMAT(1HO,1P2E15.5)
200      CONTINUE
        STOP
        END
```

Definition of Symbols.

K = overall equilibrium constant

K23 = k_{23}

K32 = k_{32}

K1 = equilibrium constant of the first step

K2 = equilibrium constant of the second step

A = monomer concentration

Y = $\tau^{-1}_{observed}$

RIS = $\tau^{-1}_{observed} - \tau^{-1}_{calculated}$

OLDVAR = old variance

VAR = variance

YC = $\tau^{-1}_{calculated}$

S1 = $\Sigma(\partial Y/\partial k_{23})^2$

S2 = $\Sigma(\partial Y/\partial k_{23})(\partial Y/\partial k_{32})$

S3 = $\Sigma(\partial Y/\partial k_{32})^2$

S4 = $\Sigma(\partial Y/\partial k_{23})(Y - YC)$

S5 = $\Sigma(\partial Y/\partial k_{32})(Y - YC)$

LIST OF REFERENCES

1. Bineau, Ann. Chim. Phys., 18, 228 (1846).

2. G. Allen and E. F. Caldin, Quart. Rev., 7, 255 (1953).

3. G. C. Pimentel and A. L. McClellan, "The Hydrogen Bond," W. H. Freeman and Co., San Francisco, Calif., 1960.

4. J. Davis, K. Pitzer, and C. N. R. Rao, J. Phys. Chem., 64, 1744 (1960).

5. C. N. R. Rao, "Chemical Applications of Infrared Spectroscopy," Academic Press Inc., New York, N. Y., 1963.

6. J. A. Pople, H. J. Bernstein and W. G. Schneider, "High Resolution Nuclear Magnetic Resonance," McGraw-Hill Co., New York, N. Y., 1959.

7. M. Tsuboi, Bull. Chem. Soc. Japan, 22, 215 (1949).

8. M. Tsuboi, Ibid., 24, 75 (1951).

9. S. E. Darman and G. B. B. M. Sutherland, Nature, 164, 440 (1949).

10. W. Klemperer, M. W. Cronyn, A. H. Maki and G. C. Pimentel, J. Amer. Chem. Soc. 76, 5846 (1954).

11. R. C. Lord and T. J. Porro, Z. Electrochem., 64, 672 (1960).

12. C. Y. S. Chen and C. A. Swenson, J. Phys. Chem., 73, 1363 (1969).

13. C. Y. S. Chen and C. A. Swenson, Ibid., 73, 2999 (1969).

14. J. E. Piercy and J. Lamb, Trans. Faraday Soc., 46, 930 (1956).

15. W. Maier, Z. Elektrochem., 64, 132 (1960).

16. W. Maier, J. Chim. Phys., 61, 239 (1964).

17. J. Rassing, Q Østerberg and T. A. Bak, Acta Chem. Scand., 21, 1443 (1967).

18. M. Musa and M. Eisner, J. Chem. Phys., 30, 227 (1959).

19. F. O. Goodman, J. Chem. Phys., 34, 1585 (1961).

20. F. Garland, Ph.D. Thesis, University of Maryland, 1968.

21. K. Bergmann, M. Eigen, and L. de Maeyer, Ber. Bunsenges. Phys. Chem. 67, 819 (1963).

22. G. G. Hammes and H. Olin Spivey, J. Amer. Chem. Soc., 88, 1621 (1966).

23. J. Rassing, accepted for publication in Acta. Chem. Scand.

24. J. Rassing and Ole Østerberg, Acta. Chem. Scand., 23, 693 (1969).

25. L. de Maeyer, M. Eigen, and J. Suarez, J. Amer. Chem. Soc., 90, 3157 (1968).

26. M. Eigen and L. de Maeyer in "Technique of Organic Chemistry," 2nd ed., (S. Friess, E. Lewis and A. Weissberger, Eds.), Interscience Publishers, New York, N. Y., 1963. Vol. VIII, Part II, Chapter XVIII.

27. K. Kustin, D. Shear and D. Kleitman, J. Theoret. Biol., 9, 186 (1965).

28. G. W. Castellan, Ber. Bunsenges., 67, 898 (1963).

29. G. Schwarz, Rev. Mod. Phys., 40, 206 (1968).

30. G. Czerlinski, J. Theoret. Biol., 7, 435 (1964).

31. J. Rassing and H. Lassen, Acta Chem. Scand., 23, 1007 (1969).

32. K. F. Herzfeld and T. A. Litovitz, "Absorption and Dispersion of Ultrasonic Waves," Academic Press, New York, 1959.

33. Benson Carlin, "Ultrasonics," McGraw-Hill Inc., New York, N. Y., 1949.

34. J. Lamb in "Physical Acoustics," (W. P. Mason, Ed.), Academic Press, New York, 1965. Vol. II, Part A, Chapter 4.

35. Valpey Crystal Corp., Holliston, Mass.

36. D. Tabuchi, Z. Elektrochem., 64, 141 (1960).

37. J. Lamb and J. M. M. Pinkerton, Proc. Roy. Soc., 199 A, 114 (1949).

38. M. V. Smoluchowski, Z. Physik. Chem., 92, 129 (1917).

39. J. Timmermans, "Physico-Chemical Constants," Elsevier Publishing Co., Inc., New York, 1950.

40. "Experimental Statistics," Handbook 91, U. S. Department of Commerce, National Bureau of Standards, 1963. Chapters 5 and 6.

41. R. Kay, J. Amer. Chem. Soc., 82, 2099 (1960).

VITA

Name: Mostafa Mahmoud Emara.

Permanent Address: 15 Kamal Eldin Salah Street, Semuha, Alexandria, Egypt (U.A.R.)

Degree and Date to be conferred: Ph.D., 1971.

Date of birth: March 23, 1942.

Place of birth: Abu. Hommos, Behera, U.A.R.

Secondary education: Damanhour, 1958.

Collegiate institutions attended	Dates	Degree	Date of Degree
Alexandria University	1958-1962	B.S.	1962
Polytechnic Institute of Brooklyn	1964-1967	M.S.	1967
University of Maryland	1967-1970	Ph.D.	1970

Major: Physical Chemistry.

Minors: Inorganic/Organic Chemistry, Mathematics.

Positions held:

Instructor, Faculty of Science, Cairo University (1962-1963).

Instructor, Faculty of Science, Alexandria University (1963-1964).

Teaching Assistant, University of Maryland (1967-1968).

Research Assistant, University of Maryland (1968-1970).